Preface

Akin to B-splines, the appeal of subdivision surfaces reaches across disciplines from mathematics to computer science and engineering. In particular, subdivision surfaces have had a dramatic impact on computer graphics and animation over the last 10 years: the results of a development that started three decades ago can be viewed today at movie theaters, where feature length movies cast synthetic characters 'skinned' with subdivision surfaces. Correspondingly, there is a rich, ever-growing literature on its fundamentals and applications.

Yet, as with every vibrant new field, the lack of a uniform notation and standard analysis tools has added unnecessary, at times inconsistent, repetition that obscures the simplicity and beauty of the underlying structures. One goal in writing this book is to help shorten introductory sections and simplify proofs by proposing a standard set of concepts and notation.

When we started writing this book in 2001, we felt that the field had sufficiently settled for standardization. After all, Cavaretta, Dahmen, and Micchelli's monograph [CDM91] had appeared 10 years earlier and we could build on the habilitation of the second author as well as a number of joint papers. But it was only in the process of writing and seeing the issues in conjunction, that structures and notation became clearer. In fact, the length of the book repeatedly increased and decreased, as key concepts and structures emerged.

Chapter 2/15, for example, was a late addition, as it became clear that the differential geometry for singular parameterizations, of continuity, smoothness, curvature, and injectivity, must be established upfront and in generality to simplify the exposition and later proofs. By contrast, the key definition of subdivision surfaces as splines with singularities, in Chap. 3/39, was a part of the foundations from the outset. This point of view implies a radical departure from any focus on control nets and instead places the main emphasis on nested surface rings, as explained in Chap. 4/57. Careful examination of existing proofs led to the explicit formulation of a number of assumptions, in Chap. 5/83, that must hold when discussing subdivision surfaces in generality. Conversely, placing these key assumptions upfront, shortened the presentation considerably. Therefore, the standard examples of subdivision algorithms reviewed in Chap. 6/109 are presented with a new, shorter and simpler analysis than in earlier publications. Chapters 7/125 and 8/157 were triggered by very recent, new insights and results and partly contain unpublished material. The suitability of the major known subdivision algorithms for engineering design was at the heart of the investigations into the shape of subdivision surfaces in Chap. 7/125. The shortcomings of the standard subdivision algorithms discovered in the process forced a renewed search for an approach to subdivision capable of meeting shape and higher-order continuity requirements. Guided subdivision was devised in response. The second part of Chap. 7/125 recasts this class of subdivision algorithms in a more abstract form that may be used as a prototype for a number of new curvature continuous subdivision algorithms. The first part of Chap. 8/157 received a renewed impetus from a recent stream of publications aimed at predicting the distance of a subdivision surface from their geometric control structures after some m refinement steps. The introduction of proxy surfaces and the distance to the corresponding subdivision surface subsumes this set of questions and provides a framework for algorithm-specific optimal estimates. The second part of Chap. 8/157 grew out of the surprising observation that the Catmull–Clark subdivision can represent the same sphere-like object starting from any member of a whole family of initial control configurations. The final chapter, Chap. 9/175, shows that a large variety of subdivision algorithms is fully covered by the exposition in the book. But it also outlines the limits of our current knowledge and opens a window to the fascinating forms of subdivision currently beyond the canonical theory and to the many approaches still awaiting discovery.

As a monograph, the book is primarily targeted at the subdivision community, including not only researchers in academia, but also practitioners in industry with an interest in the theoretical foundations of their tools. It is not intended as a course text book and contains no exercises, but a number of worked out examples. However, we aimed at an exposition that is as self-contained as possible, requiring, we think, only basic knowledge of linear algebra, analysis or elementary differential geometry. The book should therefore allow for independent reading by graduate students in mathematics, computer science, and engineering looking for a deeper understanding of subdivision surfaces or starting research in the field.

Two valuable sources that complement the formal analysis of this book are the SIGGRAPH course notes [ZS00] compiled by Schröder and Zorin, and the book ‘Subdivision Methods for Geometric design’ by Warren and Weimer [WW02]. The notes offer the graphics practitioner a quick introduction to algorithms and their implementation and the book covers a variety of interesting aspects outside our focus; for example, a connection to fractals, details of the analysis of univariate algorithms, variational algorithms based on differential operators and observations that can simplify implementation.

We aimed at unifying the presentation, placing for example *bibliographical notes* at the end of each core chapter to point out relevant and original references. In addition to these, we included a large number of publications on subdivision surfaces in the reference section. Of course, given the ongoing growth of the field, these notes cannot claim completeness. We therefore reserved the internet site

`www.subdivision-surface.org`

for future pointers and additions to the literature and theme of the book, and, just possibly, to mitigate any damage of insufficient proof reading on our part.

It is our pleasure to thank at this point our colleagues and students for their support: *Jianhua Fan*, *Ingo Ginkel*, *Jan Hakenberg*, *René Hartmann*, *Kęstutis Karčiauskas*, *Minho Kim*, *Ashish Myles*, *Tianyun Lisa Ni*, *Andy LeJeng Shiue*, *Georg Umlauf*, and *Xiaobin Wu* who worked with us on subdivision surfaces over many years. *Jan Hakenberg*, *René Hartmann*, *Malcolm Sabin*, *Neil Stewart*, and *Georg Umlauf* helped to enhance the manuscript by careful proof-reading and providing constructive feedback. *Malcolm Sabin* and *Georg Umlauf* added valuable material for the bibliographical notes. *Nira Dyn* and *Malcolm Sabin* willingly contributed two sections to the introductory chapter, and it was again *Malcolm Sabin* who shared his extensive list of references on subdivision which formed the starting point of our bibliography. *Chandrajit Bajaj* generously hosted a retreat of the authors that brought about the final structure of the book. Many thanks to you all! The work was supported by the NSF grants CCF-0430891 and DMI-0400214.

Our final thanks are reserved for our families for their support and their patience. You kept us inspired.

Chapter 7
Shape Analysis and C_2^k-Algorithms

In the preceding chapters, we have studied first order properties of subdivision surfaces in the vicinity of an extraordinary point. Now we look at second order properties, such as the Gaussian curvature or the embedded Weingarten map, which characterize shape. To simplify the setup, we assume $k \geq 2$ throughout. That is, second order partial derivatives of the patches $\mathbf{x}_j^m$ exist and satisfy the contact conditions (4.7/62) and (4.8/62) between neighboring and consecutive segments. However, most concepts are equally useful in situations where the second order partial derivatives are well defined only almost everywhere. In particular, all piecewise polynomial algorithms, such as Doo–Sabin type algorithms or Simplest subdivision, can be analyzed following the ideas to be developed now.

In Sect. 7.1/126, we apply the higher-order differential geometric concepts of Chap. 2/15 to subdivision surfaces and derive asymptotic expansions for the fundamental forms, the embedded Weingarten map, and the principal curvatures. In particular, we determine limit exponents for L^p-integrability of principal curvatures in terms of the leading eigenvalues of the subdivision matrix. The *central ring* will play a key role, just as the characteristic ring for the study for first order properties.

In Sect. 7.2/134, we can leverage the concepts to characterize fundamental shape properties. To this end, the well-known notions of ellipticity and hyperbolicity are generalized in three different ways to cover the special situation in a vicinity of the central point. Properties of the central ring reflect the local behavior, while the Fourier index $\mathcal{F}(\mu)$ of the subsubdominant eigenvalue μ of the subdivision matrix is closely related to the variety of producible shapes. In particular, $\mathcal{F}(\mu) \supset \{0, 2, n-2\}$ is necessary to avoid undue restrictions. Further, we introduce *shape charts* as a tool for summarizing, in a single image, information about the entirety of producible shape.

Conditions for C_2^k-algorithms are discussed in Sect. 7.3/140. Following Theorem 2.14/28, curvature continuity is equivalent to convergence of the embedded Weingarten map. This implies that the subsubdominant eigenvalue μ must be the square of the subdominant eigenvalue λ, and the subsubdominant eigenrings must be quadratic polynomials in the components of the characteristic ring. These extremely restrictive conditions explain the difficulties encountered when trying to construct C_2^k-algorithms. In particular, they lead to a lower bound on the degree of piecewise polynomial schemes, which rules out all schemes generalizing uniform B-spline subdivision, such as the Catmull–Clark algorithm.

Section 7.4/145 presents hitherto unpublished material concerning a general principle for the construction of C_2^k-algorithms, called the *PTER-framework*. This acronym refers to the four building blocks: projection, turn-back, extension, and reparametrization. The important special case of *Guided subdivision*, which inspired that development, is presented in Sect. 7.5/149.

7.1 Higher Order Asymptotic Expansions

We focus on symmetric standard C_1^2-algorithms and assume, for simplicity of exposition, that the subdominant Jordan blocks are singletons, i.e.,

$$1 > \lambda := \lambda_1 = \lambda_2 > |\lambda_3|, \quad \ell_1 = \ell_2 = 0.$$

All subsequent arguments are easily generalized to the case of subdominant Jordan blocks of higher dimension (see Sect. 5.3/89), but the marginal extra insight does not justify the higher technical complexity. We obtain the structure

$$(1,0) \succ (\lambda,0) \sim (\lambda,0) \succ (\lambda_3,\ell_3) \sim \cdots \sim (\lambda_{\bar{q}},\ell_{\bar{q}}) \succ (\lambda_{\bar{q}+1},\ell_{\bar{q}+1})$$

for the eigenvalues, and denote by μ the common modulus of the *subsubdominant eigenvalues* and by ℓ the size[1] of the corresponding Jordan blocks minus one:

$$\mu := |\lambda_3| = \cdots = |\lambda_{\bar{q}}|, \quad \ell := \ell_3 = \cdots = \ell_{\bar{q}}.$$

Consider a subdivision surface $\mathbf{x}$ corresponding to generic initial data $\mathbf{Q}$. Following Definition 2.11/25, we denote by $\mathbf{n}^c$ the central normal, and by $(\mathbf{t}_1^c, \mathbf{t}_2^c, \mathbf{n}^c)$ an orthonormal system defining the central frame $\mathbf{F}^c$,

$$\mathbf{T}^c := \begin{bmatrix} \mathbf{t}_1^c \\ \mathbf{t}_2^c \end{bmatrix}, \quad \mathbf{F}^c := \begin{bmatrix} \mathbf{T}^c \\ \mathbf{n}^c \end{bmatrix}.$$

With (4.28/74), the *second order* asymptotic expansion of the rings $\mathbf{x}^m$ reads

$$\mathbf{x}^m \stackrel{*}{=} \mathbf{x}^c + \lambda^m \boldsymbol{\psi}[\mathbf{p}_1;\mathbf{p}_2] + \mu^{m,\ell}\mathbf{d}^m. \tag{7.1}$$

The term

$$\mathbf{d}^m := \sum_{q=3}^{\bar{q}} d_q^{m-\ell} f_q \mathbf{p}_q$$

summarizes the contribution of the subsubdominant eigencoefficients $\mathbf{p}_q$ and eigenrings f_q. The directions $d_q = \lambda_q/\mu$, as defined in (4.31/75), are numbers on the

[1] Note that the symbol ℓ does not indicate the size of the *subdominant* Jordan block, as in earlier chapters, but the size of the *subsubdominant* Jordan block.

complex unit circle, referring to the angles of the potentially complex subsubdominant eigenvalues $\lambda_3, \dots, \lambda_{\bar q}$.

According to (4.21/73), the scaling factor in (7.1/126) is $\mu^{m,\ell} = \binom{m}{\ell}\mu^{m-\ell}$ provided that $m \ge \ell$. Hence, if $\mu = 0$, the rings $\mathbf{x}^m$ become entirely flat after a few steps. To exclude this trivial situation, we assume $\mu > 0$ throughout. Appropriate asymptotic expansions of the rings of the tangential and the normal component of the transformed spline $\mathbf{x}_* = (\mathbf{x} - \mathbf{x}^c) \cdot \mathbf{F}^c$, as defined in (4.11/64), are given by

$$\boldsymbol{\xi}_*^m = (\mathbf{x}^m - \mathbf{x}^c) \cdot \mathbf{T}^c \stackrel{*}{=} \lambda^m \boldsymbol{\psi}\, [\mathbf{p}_1; \mathbf{p}_2] \cdot \mathbf{T}^c$$

and

$$z_*^m = (\mathbf{x}^m - \mathbf{x}^c) \cdot \mathbf{n}^c \stackrel{*}{=} \mu^{m,\ell} \mathbf{d}^m \cdot \mathbf{n}^c, \tag{7.2}$$

respectively. We will focus on algorithms without negative or complex directions d_q. For if, say d_3, is negative or complex then d_3^m oscillates, and if the corresponding coefficient $\mathbf{p}_3 \cdot \mathbf{n}^c$ dominates then z_*^m repeatedly attains positive and negative values as m is growing. In other words, the rings $\mathbf{x}^m$ repeatedly cross the central tangent plane, an undesirable behavior for applications. We therefore focus on algorithms with the following properties:

Definition 7.1 (Algorithm of type (λ, μ, ℓ)). A subdivision algorithm (A, G) is said to be of *type* (λ, μ, ℓ), if

- (A, G) is a symmetric standard C_1^2-algorithm, and
- the *subsubdominant Jordan blocks* have a unique positive eigenvalue,

$$\mu := \lambda_3 = \cdots = \lambda_{\bar q} > 0, \quad \ell := \ell_3 = \cdots = \ell_{\bar q}, \quad (\mu, \ell) \succ (\lambda_{\bar q+1}, \ell_{\bar q+1}).$$

Let us briefly discuss some simple consequences of the assumptions made here: In view of Definition 5.3/84, we have a double subdominant eigenvalue,

$$1 > \lambda := \lambda_1 = \lambda_2 > |\lambda_3|, \quad \ell_1 = \ell_2 = 0.$$

Further, by Definition 5.9/89 and Theorem 5.18/101, the Fourier index of λ must be

$$\mathcal{F}(\lambda) = \{1, n-1\}$$

to ensure that the characteristic ring $\boldsymbol{\psi}$ is uni-cyclic.

For an algorithm of type (λ, μ, ℓ),

$$\begin{aligned} \boldsymbol{\xi}_*^m &\stackrel{*}{=} \lambda^m \overline{\boldsymbol{\xi}}, \quad \overline{\boldsymbol{\xi}} := \boldsymbol{\psi} L, \quad L := [\mathbf{p}_1; \mathbf{p}_2] \cdot \mathbf{T}^c \\ z_*^m &\stackrel{*}{=} \mu^{m,\ell} \overline{z}, \quad \overline{z} := \mathbf{d}^m \cdot \mathbf{n}^c = \sum_{q=3}^{\bar q} f_q \mathbf{p}_q \cdot \mathbf{n}^c. \end{aligned} \tag{7.3}$$

The planar ring $\overline{\boldsymbol{\xi}} = \boldsymbol{\psi} L$ is an affine image of the characteristic ring. By (2.5/17),

$$^{\times}D\overline{\boldsymbol{\xi}} = {}^{\times}D\boldsymbol{\psi}\, \det L, \tag{7.4}$$

i.e., it is regular and injective if and only if L is invertible. From

$$[\mathbf{p}_1; \mathbf{p}_2; \mathbf{n}^{\mathrm{c}}] \cdot \mathbf{F}^{\mathrm{c}} = \begin{bmatrix} L & 0 \\ 0 & 1 \end{bmatrix}$$

we conclude that

$$\det L = \det[\mathbf{p}_1; \mathbf{p}_2; \mathbf{n}^{\mathrm{c}}] = \pm\|\mathbf{p}_1 \times \mathbf{p}_2\|. \tag{7.5}$$

Hence, L is invertible if and only if $\mathbf{p}_1$ and $\mathbf{p}_2$ are linearly independent. In particular, $\bar{\boldsymbol{\xi}}$ is regular and injective for generic initial data. Since, by assumption, $d_q = 1$ for $q = 3, \ldots, \bar{q}$, the factors $d_q^{m-\ell}$ in the definition of $\mathbf{d}^m$ disappear so that the real-valued ring $\bar{z} = \mathbf{d}^m \cdot \mathbf{n}^{\mathrm{c}}$, appearing in the formula for z_*^m, is independent of m. Together, we find the expansion

$$\mathbf{x}_* = (\mathbf{x}^m - \mathbf{x}^{\mathrm{c}}) \cdot \mathbf{F}^{\mathrm{c}} \stackrel{*}{=} \left[\lambda^m \bar{\boldsymbol{\xi}},\ \mu^{m,\ell}\bar{z}\right] = \left[\bar{\boldsymbol{\xi}},\ \bar{z}\right] \operatorname{diag}(\lambda^m, \lambda^m, \mu^{m,\ell}), \tag{7.6}$$

where the asymptotic equivalence of sequences is understood component-wise. That is, the tangential and the normal component are specified exactly up to terms of order $o(\lambda^m)$ and $o(\mu^{m,\ell})$, respectively. Equation (7.6/128) shows that, up to a Euclidean motion, the rings $\mathbf{x}^m$ are asymptotically just scaled copies of the surface $\left[\bar{\boldsymbol{\xi}}, \bar{z}\right]$. For the forthcoming investigation of curvature and shape properties, this surface plays a most important role.

Definition 7.2 (Central ring and central spline). Consider a subdivision surface $\mathbf{x} = B\mathbf{Q} \in C^k(\mathbf{S}_n, \mathbb{R}^3)$ generated by an algorithm of type (λ, μ, ℓ) with central normal $\mathbf{n}^{\mathrm{c}}$, central frame $\mathbf{F}^{\mathrm{c}}$, and eigencoefficients $\mathbf{P} := V^{-1}\mathbf{Q}$. Let $\bar{\mathbf{P}}$ be a vector of points in $\mathbb{R}^3$ with the same block structure as $\mathbf{P}$, see (4.25/74), and all entries zero except for

$$\bar{\mathbf{p}}_0 := \mathbf{0}, \quad [\bar{\mathbf{p}}_1; \bar{\mathbf{p}}_2] := [\mathbf{p}_1; \mathbf{p}_2] \cdot \mathbf{F}^{\mathrm{c}}, \quad \bar{\mathbf{p}}_q^0 := [0,\ \mathbf{p}_q \cdot \mathbf{n}^{\mathrm{c}}], \quad q = 3, \ldots, \bar{q}.$$

The *central ring* $\bar{\mathbf{r}}$ and the *central spline* $\bar{\mathbf{x}}$ corresponding to $\mathbf{x}$ are defined by

$$\bar{\mathbf{r}} := F\bar{\mathbf{P}} \in C^k(\mathbf{S}_n^0, \mathbb{R}^3), \quad \bar{\mathbf{x}} := BV\bar{\mathbf{P}} \in C^k(\mathbf{S}_n, \mathbb{R}^3).$$

Recalling (7.3/127), we find $[\bar{\mathbf{p}}_1; \bar{\mathbf{p}}_2] = [L, 0]$ and

$$\bar{\mathbf{r}} := \left[\bar{\boldsymbol{\xi}},\ \bar{z}\right].$$

Further, we observe the following: According to the structure defined in (4.25/74), $\bar{\mathbf{p}}_q^0$ is the *first* entry in the block $\bar{\mathbf{P}}_q$ of $\bar{\mathbf{P}}$, while $\mathbf{p}_q = \mathbf{p}_q^\ell$ is the *last* entry in the block $\mathbf{P}_q$. Hence, when computing the ring $\bar{\mathbf{x}}^m = FJ^m\bar{\mathbf{P}}$ of the central spline, the summands with index $q = 3, \ldots, \bar{q}$ are $F_q J_q^m \bar{\mathbf{P}}_q = \mu^m f_q \bar{\mathbf{p}}_q^0$. We obtain

$$\bar{\mathbf{x}}^m = \left[\lambda^m \bar{\boldsymbol{\xi}},\ \mu^m \sum_{q=3}^{\bar{q}} f_q \bar{\mathbf{p}}_q^0\right] = \bar{\mathbf{r}} \operatorname{diag}(\lambda^m, \lambda^m, \mu^m)$$

and see that these rings are scaled copies of $\bar{\mathbf{r}}$. The central point and the central normal of $\bar{\mathbf{x}}$ are given by

$$\bar{\mathbf{x}}^{\mathrm{c}} = \bar{\mathbf{p}}_0 = \mathbf{0}, \quad \bar{\mathbf{n}}^{\mathrm{c}} = \frac{\bar{\mathbf{p}}_1 \times \bar{\mathbf{p}}_2}{\|\bar{\mathbf{p}}_1 \times \bar{\mathbf{p}}_2\|} = \mathbf{e}_3 := [0,0,1], \tag{7.7}$$

respectively.

Unlike the characteristic ring, the central ring depends on the initial data via the eigencoefficients $\mathbf{p}_1, \ldots, \mathbf{p}_{\bar{q}}$ in (7.3/127). If these data are generic then the central ring is regular, i.e., ${}^{\times}\!D\bar{\mathbf{r}} \neq \mathbf{0}$. More precisely, using (7.4/127), one easily shows that

$$\|{}^{\times}\!D\bar{\mathbf{r}}\| \geq |{}^{\times}\!D\bar{\boldsymbol{\xi}}| = {}^{\times}\!D\psi \,|\det L|,$$

where we recall that, by definition, ${}^{\times}\!D\psi > 0$ for a standard algorithm. We start with a lemma concerning the first and second fundamental form.

Lemma 7.3 (Asymptotic expansion of fundamental forms). *For generic initial data consider a subdivision surface $\mathbf{x} = B\mathbf{Q} \in C^k(\mathbf{S}_n, \mathbb{R}^3)$ with segments $\mathbf{x}_j^m$ generated by a subdivision algorithm of type (λ, μ, ℓ). Then we obtain the following asymptotic expansions:*

- *The first fundamental form of $\mathbf{x}_j^m$ is a symmetric matrix $I_j^m \in C^{k-1}(\boldsymbol{\Sigma}^0, \mathbb{R}^{2\times 2})$ with*

$$I_j^m \stackrel{*}{=} \lambda^{2m} I_j, \quad \textit{where} \quad I_j := D\bar{\boldsymbol{\xi}}_j \cdot D\bar{\boldsymbol{\xi}}_j. \tag{7.8}$$

- *There exists $\bar{m}$ such that the inverse $(I_j^m)^{-1}$ exists for all $m \geq \bar{m}$, $j \in \mathbb{Z}_n$, and satisfies*

$$(I_j^m)^{-1} \stackrel{*}{=} \lambda^{-2m} I_j^{-1}. \tag{7.9}$$

- *Let $\bar{I}_j$ and $\bar{I\!I}_j$ denote the first and second fundamental form of the segments of the central ring $\bar{\mathbf{r}}$. The second fundamental form of $\mathbf{x}_j^m$ is a symmetric matrix $I\!I_j^m \in C^{k-2}(\boldsymbol{\Sigma}^0, \mathbb{R}^{2\times 2})$ with*

$$I\!I_j^m \stackrel{*}{=} \mu^{m,\ell}\, I\!I_j, \quad \textit{where} \quad I\!I_j := \sqrt{\frac{\det \bar{I}_j}{\det I_j}}\, \bar{I\!I}_j. \tag{7.10}$$

Proof. The first formula, (7.8/129), follows immediately from the definition $I_j^m := D\mathbf{x}_j^m \cdot D\mathbf{x}_j^m$ and the expansion

$$D\mathbf{x}_j^m \stackrel{*}{=} \lambda^m D\bar{\boldsymbol{\xi}}_j \mathbf{T}_j^{\mathrm{c}}. \tag{7.11}$$

To compute $(I_j^m)^{-1}$, we note that the inverse of any (2×2)-matrix M with $\det M \neq 0$ can be expressed in the form

$$M^{-1} = \frac{1}{\det M}\,(C \cdot M) \cdot C, \quad \text{where} \quad C := \begin{bmatrix} 0 & -1 \\ 1 & 0 \end{bmatrix},$$

where we recall that the dot operator transposes its right argument. Now, using (7.4/127),

$$\det I^m_j \stackrel{*}{=} \lambda^{4m} \det I_j = \lambda^{4m} ({}^{\times}D\bar{\boldsymbol{\xi}}_j)^2 = \lambda^{4m} ({}^{\times}D\boldsymbol{\psi}_j)^2 (\det L)^2. \qquad (7.12)$$

By (7.5/128), $(\det L)^2 = \|\mathbf{p}_1 \times \mathbf{p}_2\|^2$ does not vanish for generic initial data, while $({}^{\times}D\boldsymbol{\psi}_j)^2 \geq c_j > 0$ for some constant c_j by regularity of $\boldsymbol{\psi}_j$, compactness of the domain $\boldsymbol{\Sigma}^0$, and continuity of ${}^{\times}D\boldsymbol{\psi}_j$. Hence, the right hand side in the last display is bounded away from zero so that there exists an integer $\bar{m}$ with $\det I^m_j > 0$ for all $m \geq \bar{m}$, $j \in \mathbb{Z}_n$, and

$$(\det I^m_j)^{-1} \stackrel{*}{=} \lambda^{-4m} (\det I_j)^{-1}. \qquad (7.13)$$

As claimed in (7.9/129), we obtain

$$(I^m_j)^{-1} = \frac{1}{\det I^m_j} (C \cdot I^m_j) \cdot C \stackrel{*}{=} \frac{\lambda^{-2m}}{\det I_j} (C \cdot I_j) \cdot C = \lambda^{-2m} I_j^{-1}.$$

To prove (7.10/129), we conclude from (7.6/128)

$$\det[D_i D_k \mathbf{x}^m_j; D\mathbf{x}^m_j] \stackrel{*}{=} \lambda^{2m} \mu^{m,\ell} \det[D_i D_k \bar{\mathbf{x}}_j; {}^{\times}D\bar{\mathbf{x}}_j].$$

Then, by comparing the components

$$(II^m_j)_{i,k} = \frac{\det[D_i D_k \mathbf{x}^m_j; D\mathbf{x}^m_j]}{\sqrt{\det I^m_j}}, \quad (II^{\mathrm{c}}_j)_{i,k} = \frac{\det[D_i D_k \bar{\mathbf{x}}_j; D\bar{\mathbf{x}}_j]}{\sqrt{\det I^{\mathrm{c}}_j}}$$

of II^m_j and II^{c}_j according to (2.8/19) and using (7.13/130), we obtain the given expansion. □

In the following, we will assume without further notice that, if required, $m \geq \bar{m}$ so that I^m_j is invertible. With the help of the expansions for the fundamental forms, we are now able to derive the expansion for the embedded Weingarten map of the rings.

Theorem 7.4 (Asymptotic expansion of $\mathbf{W}^m$). Under the assumptions of Lemma 7.3/129, the embedded Weingarten maps of the rings $\mathbf{x}^m \in C^k(\mathbf{S}^0_n, \mathbb{R}^3)$ are rings $\mathbf{W}^m \in C^{k-2}(\mathbf{S}^0_n, \mathbb{R}^{3\times 3})$ with

$$\mathbf{W}^m \stackrel{*}{=} \varrho^{m,\ell} (\mathbf{T}^{\mathrm{c}})^{\mathrm{t}} W \mathbf{T}^{\mathrm{c}}, \quad \varrho := \frac{\mu}{\lambda^2}, \qquad (7.14)$$

where W is a symmetric (2×2)-matrix with segments

$$W_j := (D\bar{\boldsymbol{\xi}}_j)^{-1} II_j \cdot (D\bar{\boldsymbol{\xi}}_j)^{-1}, \quad j \in \mathbb{Z}_n. \qquad (7.15)$$

Moreover, consecutive rings $\mathbf{W}^m, \mathbf{W}^{m+1}$ join smoothly in the sense that the segments satisfy the contact conditions (4.8/62) up to order $k-2$.

Proof. Recalling Definition 2.4/20, and using (7.11/129) and (7.9/129), the pseudo-inverse of $D\mathbf{x}^m_j$ is

$$(D\mathbf{x}_j^m)^+ \stackrel{*}{=} \lambda^{-m}\big((\mathbf{T}^c)^t \cdot D\overline{\boldsymbol{\xi}}_j\big)(D\overline{\boldsymbol{\xi}}_j \cdot D\overline{\boldsymbol{\xi}}_j)^{-1} = \lambda^{-m}(\mathbf{T}^c)^t(D\overline{\boldsymbol{\xi}}_j)^{-1}.$$

Together with (7.10/129), we find the desired expansion. The C^{k-2}-contact of consecutive and neighboring segments is shown as follows. Using the fractional power embedding $\boldsymbol{\pi}$, as introduced in Example 3.10, we define the reparametrized surface $\tilde{\mathbf{x}} := \mathbf{x} \circ \boldsymbol{\pi}^{-1}$, which is not a spline, but an almost regular standard C_0^k-surface. Its embedded Weingarten map $\tilde{\mathbf{W}}$ is well defined and C^{k-2} away from the origin. Because the images of $\mathbf{x}$ and $\tilde{\mathbf{x}}$ coincide, so do the corresponding embedded Weingarten maps, see Theorem 2.5/22. Hence, smooth contact of the segments $\mathbf{W}_j^m$ follows from smoothness of $\tilde{\mathbf{W}}$. □

Now, using the formulas (2.11/22) and the identities

$$\operatorname{trace}\big((\mathbf{T}^c)^t\, W \mathbf{T}^c\big) = \operatorname{trace} W, \quad \|(\mathbf{T}^c)^t\, W \mathbf{T}^c\|_F = \|W\|_F,$$

we easily find the asymptotic expansions

$$\kappa_M^m \stackrel{*}{=} \frac{\varrho^{m,\ell}}{2} \operatorname{trace} W \tag{7.16}$$

for the mean curvature, and

$$\kappa_G^m \stackrel{*}{=} \frac{(\varrho^{m,\ell})^2}{2}(\operatorname{trace}^2 W - \|W\|_F^2) = (\varrho^{m,\ell})^2 \det W \tag{7.17}$$

for the Gaussian curvature. Let us derive two further asymptotic formulas from these expansions. First, we see immediately that the principal curvatures $\kappa_{1,2}^m$ of $\mathbf{x}^m$ and the eigenvalues $\kappa_{1,2}^W$ of W are related by

$$\kappa_i^m \stackrel{*}{=} \varrho^{m,\ell}\kappa_i^W, \quad i \in \{1, 2\}. \tag{7.18}$$

Second, let $\bar{\kappa}_G := \det \bar{I\!I}/\det \bar{I}$ denote the Gaussian curvature of the central ring. Then, with the definitions (7.10/129) of $I\!I$ and (7.15/130) of W, we further find using $|^{\times}D\overline{\boldsymbol{\xi}}| = \sqrt{\det I}$

$$\kappa_G^m \stackrel{*}{=} \left(\varrho^{m,\ell}\,\frac{\det \bar{I}}{\det I}\right)^2 \bar{\kappa}_G. \tag{7.19}$$

In particular, this formula shows that elliptic and hyperbolic points of the central ring $\bar{\mathbf{r}}$ correspond to elliptic and hyperbolic points of the rings $\mathbf{x}^m$, respectively, for sufficiently large m. Of course, parabolic points of $\bar{\mathbf{r}}$ do not admit a similar conclusion.

The preceding formulas, and in particular (7.18/131), indicate that the ratio $\varrho = \mu/\lambda^2$ together with the dimension ℓ of the subsubdominant Jordan block governs the limit behavior of the principal curvatures of the rings. Clearly, $\varrho < 1$ implies convergence to 0, while $(\varrho, \ell) = (1, 0)$ guarantees boundedness. However, it is not obvious that $(\varrho, \ell) \succ (1, 0)$ necessarily causes divergence since both eigenvalues of W could still be 0. This case is excluded by the following lemma.

Lemma 7.5 (Generically, $W \neq 0$). *For generic initial data* $\mathbf{P}$*, the matrix* W *does not vanish identically.*

Proof. Let us assume that $W_j = (D\bar{\boldsymbol{\xi}}_j)^{-1} II_j \cdot (D\bar{\boldsymbol{\xi}}_j)^{-1} = 0$. Because $\bar{\boldsymbol{\xi}}$ is regular for generic initial data, we have $II_j = \bar{II}_j = 0$ so that the principal curvatures of the central ring vanish identically. This is possible only if the image of $\bar{\mathbf{r}}$ is contained in a plane. Now, we consider the central spline $\bar{\mathbf{x}}$. As we have shown above, its rings $\bar{\mathbf{x}}^m$ are scaled copies of $\bar{\mathbf{r}}$, hence planar, too. Because $\bar{\mathbf{x}}$ is continuous and normal continuous, the image of $\bar{\mathbf{x}}$ must be a subset of a single plane. In view of (7.7/129), this must be the xy-plane,

$$\bar{\mathbf{r}} \cdot \mathbf{e}_3 = \bar{z} = \sum_{q=3}^{\bar{q}} f_q \, \mathbf{p}_q \cdot \mathbf{n}^{\mathrm{c}} = 0.$$

By Lemma 4.22/78, the eigenrings f_q are linearly independent, implying $\mathbf{p}_q \cdot \mathbf{n}^{\mathrm{c}} = 0$ and $\det[\mathbf{p}_1; \mathbf{p}_2; \mathbf{p}_q] = 0$ for all $q = 3, \ldots, \bar{q}$. This, however, contradicts the assumption that the initial data $\mathbf{P}$ be generic, see Definition 5.1/84. □

As a consequence of the lemma, we can be sure that the factor $\varrho^{m,\ell}$ in the asymptotic expansion (7.18/131) of the principal curvatures provides not only an upper bound. In fact, it describes the precise asymptotic behavior of at least one out of κ_1^m and κ_2^m since, for generic initial data, at least one eigenvalue of W is non-zero. For that reason, the following critical exponents for L^p-integrability of principal curvatures cannot be improved. We define the L^p-norm $\|\kappa\|_{p,\bar{m}}$ of a spline κ, built from rings κ^m, as the sum of integrals over all surface rings $\mathbf{x}^m$ with index $m \geq \bar{m}$, by

$$\|\kappa\|_{p,\bar{m}}^p := \sum_{m \geq \bar{m}} \int |\kappa|^p \, d\mathbf{x}^m = \sum_{m \geq \bar{m}} \sum_{j \in \mathbb{Z}_n} \int_{\boldsymbol{\Sigma}^0} |\kappa(s,t,j)|^p \, \|{}^{\times}D\mathbf{x}^m\| \, dsdt.$$

The space of all functions κ for which $\|\kappa\|_{p,\bar{m}}$ is well defined and finite for sufficiently large $\bar{m}$ is denoted by L^p_{loc}. Then the following theorem holds and is illustrated in Fig. 7.1/133.

Theorem 7.6 (Curvature integrability). *For generic data, let* $\mathbf{x} \in C^k(\mathbf{S}_n, \mathbb{R}^3)$ *be a subdivision surface with principal curvatures* $\kappa_i, i \in \{1,2\}$*. Then, for sufficiently large* $\bar{m}$ *and* $m \geq \bar{m}$*, the rings* κ_i^m *are well-defined. Furthermore,* $\kappa_i \in L^p_{\mathrm{loc}}$ *for all* p *with*

- $p < \frac{2\ln\lambda}{2\ln\lambda - \ln\mu}$*, if* $\mu > \lambda^2$*;*
- $p < \infty$*, if* $\mu = \lambda^2$ *and* $\ell > 0$*;*
- $p \leq \infty$*, if* $(\mu, \ell) \preccurlyeq (\lambda^2, 0)$*.*

In any case, $\kappa_i \in L^2_{\mathrm{loc}}$*.*

Proof. The principal curvatures κ_i^m are well-defined and continuous if $\det I^m > 0$. Now, the asymptotic expansion (7.12/130) guarantees the existence of an index $\bar{m}$ such that $\det I^m > 0$ for all $m \geq \bar{m}$. By (7.18/131), both principal curvatures are bounded

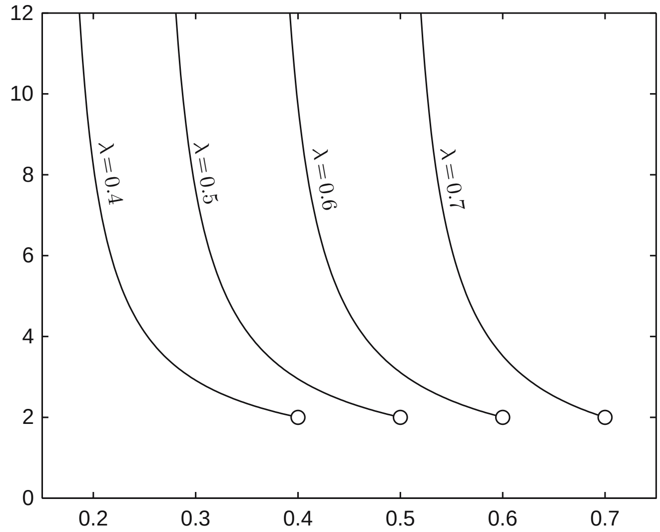

Fig. 7.1 Illustration of Theorem 7.6/132: Limit exponent p of curvature integrability plotted over subsubdominant eigenvalue μ for different values of λ.

if and only if $(\mu,\ell) \preccurlyeq (\lambda^2,0)$. Hence, it remains to consider the case $p<\infty$. We use (5.7/87), (7.4/127), and (7.5/128) to find

$$\|{}^\times\!D\mathbf{x}^m\| \stackrel{*}{=} \lambda^{2m}\|{}^\times\!D\boldsymbol{\psi}\|\,\|\mathbf{p}_1\times\mathbf{p}_2\| = \lambda^{2m}\|{}^\times\!D\bar{\boldsymbol{\xi}}\|.$$

Hence, with (7.18/131),

$$|\kappa_i^m|^p\,\|{}^\times\!D\mathbf{x}^m\| \stackrel{*}{=} (\varrho^{m,\ell})^p|\kappa_i^{\mathrm{W}}|^p\lambda^{2m}|{}^\times\!D\bar{\boldsymbol{\xi}}| \stackrel{*}{=} (m/\varrho)^{\ell p}\,r_p^m\,k_i^p,$$

where we used the abbreviations

$$r_p := \frac{\mu^p}{\lambda^{2(p-1)}} \quad\text{and}\quad k_i^p := |\kappa_i^{\mathrm{W}}|^p\,|{}^\times\!D\bar{\boldsymbol{\xi}}|.$$

Denoting the integral of the ring k_i^p by

$$K_i^p := \sum_{j\in\mathbb{Z}_n}\int_{\boldsymbol{\Sigma}^0} k_i^p(s,t,j)\,dsdt,$$

we obtain

$$\|\kappa_i\|_{p,\bar m}^p = \sum_{m\ge\bar m}\sum_{j\in\mathbb{Z}_n}\int_{\boldsymbol{\Sigma}^0}|\kappa_i^m(s,t,j)|^p\,\|{}^\times\!D\mathbf{x}^m\|\,dsdt \stackrel{*}{=} K_i^p\sum_{m\ge\bar m}(m/\varrho)^{\ell p}\,r_p^m.$$

The latter series converges if and only if $r_p<1$. For $\mu>\lambda^2$, this inequality is equivalent to p being smaller than the bound given in the first item of the theorem, while it is always satisfied for $\mu \leq \lambda^2$. The final statement, which guarantees square integrability of the principal curvatures for *any* algorithm of type (λ, μ, ℓ), follows immediately from the above results and $\mu < \ell$. □

7.2 Shape Assessment

As it will be explained in the next section, C_2^k-subdivision algorithms are hard to find, and most schemes currently in use are merely C_1^k. While many popular C_1^k-algorithms live up to the standards of Computer Graphics, they do not satisfy the higher demands arising in applications like car body design. To put it shortly, one could say that most subdivision surfaces are fair from afar, but far from being fair.

When scrutinizing subdivision surfaces by means of shaded images or curvature plots, one possibly encounters an erratic behavior of shape near the central point. It would be an oversimplification to explain these observations by just pointing to the lack of curvature continuity. Rather, it pays off to explore the deeper sources of shape deficiencies. Based on such additional insight, one can develop guidelines for tuning algorithms. Even for families of subdivision algorithms where curvature continuity is beyond reach, this may result in a significant improvement of shape.

As a motivation, consider the following facts regarding Catmull–Clark subdivision, as discussed in the preceding chapter:

- For standard weights and valence $n \geq 5$, the principal curvatures grow unboundedly when approaching the central point.
- For standard weights and valence $n \geq 5$, the generated surfaces are generically not convex.
- Even when tuning the weights α, β, γ carefully to get rid of the latter restriction, the generated surfaces sometimes reveal a *hybrid behavior*, what means that there are both elliptic and hyperbolic points in any neighborhood of the central point.

The first observation can be understood when considering the asymptotic expansion (7.18/131) derived in the preceding section: the ratio $\varrho = \mu/\lambda^2 > 1$ causes divergence of the principal curvatures. Also the second observation can be explained by spectral properties of the subdivision matrix. The subsubdominant eigenvalue μ has Fourier index $\mathcal{F}(\mu) = \{2, n-2\}$, and we will show below that this generically leads to non-convex shape. The third observation is quite subtle, and can be explained only with the help of a so-called shape chart, which summarizes properties of central rings for all possible choices of initial data.

Before we come to that point, let us start with developing concepts for classifying shape at the central point. Because, in general, the Gaussian curvature is not well defined at $\mathbf{x}^c$, we have to generalize the notions of ellipticity and hyperbolicity. We suggest three different approaches, respectively based on:

- The local intersections of the subdivision surface with its tangent plane
- The limit behavior of the Gaussian curvature
- Local quadratic approximation

We will show that in all cases the behavior of the subdivision surface is closely related to the shape of the central surface ring and, in the first and third case, to spectral properties of the subdivision matrix. For simplicity, we continue to consider algorithms of type (λ, μ, ℓ) according to Definition 7.1/127.

We start by introducing an appropriate notion of periodicity for rings.

Definition 7.7 ($\mathcal{P}$-periodicity). Let $\mathcal{P} = \{k_1, \ldots, k_q\}$ be a set of indices, which are understood modulo n. A ring $f \in C^k(\mathbf{S}_n^0, \mathbb{K})$ is called $\mathcal{P}$*-periodic*, if there exist functions $g_i, \bar{g}_i \in C^k(\boldsymbol{\Sigma}^0, \mathbb{K})$ such that its segments are given by

$$f(\cdot, j) = \sum_{i=1}^{q} \bigl(g_i \sin(2\pi k_i j/n) + \bar{g}_i \cos(2\pi k_i j/n)\bigr).$$

One easily shows that

$$\sum_{j \in \mathbb{Z}_n} f(\cdot, j) = 0 \quad \text{if} \quad 0 \notin \mathcal{P}. \tag{7.20}$$

Further, the space of $\mathcal{P}$-periodic functions is linear. The product of a $\mathcal{P}$-periodic function f and a $\mathcal{Q}$-periodic function g yields an $\mathcal{R}$-periodic function fg, where $\mathcal{R} := \mathcal{P} \pm \mathcal{Q}$ contains all sums and differences of elements of $\mathcal{P}$ and $\mathcal{Q}$.

By (5.17/99) and $\mathcal{F}(\lambda) = \{1, n-1\}$, the tangential component $\bar{\boldsymbol{\xi}} = [f_1, f_2]L$ of the central ring $\bar{\mathbf{r}}$ is $\{1, n-1\}$-periodic, while the third component $\bar{z} = \sum_q f_q\, \mathbf{p}_q \cdot \mathbf{n}^c$ is $\mathcal{F}(\mu)$-periodic.

Now, we introduce three variants on the notion of an elliptic or hyperbolic point, which apply to the special situation at the central point. As a first approach, let us consider a non-parabolic point of a regular C^2-surface. If it is elliptic, then the surface locally lies on one side of the tangent plane. By contrast, if it is hyperbolic, then the surface intersects the tangent plane in any neighborhood. This basic observation motivates the following generalization. It involves the notion of the *central tangent plane* which is the plane perpendicular to $\mathbf{n}^c$ through the point $\mathbf{x}^c$.

Definition 7.8 (Sign-type). The central point $\mathbf{x}^c$ of a subdivision surface $\mathbf{x}$ is called

- *elliptic in sign* if, in a sufficiently small neighborhood of $\mathbf{x}^c$, the subdivision surface intersects the central tangent plane only in $\mathbf{x}^c$;
- *hyperbolic in sign*, if in any neighborhood of $\mathbf{x}^c$ the subdivision surface has points on both sides of the central tangent plane.

This classification defines a minimum standard for subdivision surfaces: any high-quality algorithm should be able to generate both sign-types in order to cover basic shapes. The sign-type can be established by looking at the third component of the central ring.

Theorem 7.9 (Central surface and sign-type). *Let $\bar{\mathbf{r}} = [\bar{\boldsymbol{\xi}}, \bar{z}]$ be the central ring of the subdivision surface* $\mathbf{x}$.

- *If $\bar{z} > 0$ or $\bar{z} < 0$, then $\mathbf{x}^c$ is elliptic in sign.*
- *If $\bar{z}$ changes sign, then $\mathbf{x}^c$ is hyperbolic in sign.*

Proof. Intersections of $\mathbf{x}$ and the central tangent plane correspond to zeros of the normal component z_* of the transformed spline surface $\mathbf{x}_*$. According to (7.2/127) and (7.6/128), its rings z_*^m satisfy

$$z_*^m = (\mathbf{x}^m - \mathbf{x}^c) \cdot \mathbf{n}^c \overset{*}{=} \mu^{m,\ell}\overline{z},$$

and the assertion follows easily. □

The last display implies more than is stated in the theorem. We see that the sign map of z_*^m is equivalent to the sign map of $\overline{z}$ in an asymptotic way. Thus, the distribution of signs of the normal component z_* can be studied with the help of the central ring, except for points corresponding to zeros of $\overline{z}$. The next theorem relates the sign-type and the Fourier index of the subsubdominant eigenvalue.

Theorem 7.10 (Fourier index and sign-type). *For generic initial data, the central point* $\mathbf{x}^c$ *is hyperbolic in sign unless* $0 \in \mathcal{F}(\mu)$.

Proof. The function $\overline{z}$ is $\mathcal{F}(\mu)$-periodic. Hence, if $0 \notin \mathcal{F}(\mu)$, the sum of its segments vanishes, $\sum_{j\in\mathbb{Z}_n} \overline{z}_j = 0$. Since $\overline{z} \neq 0$ for generic initial data, it has to have positive and negative function values. □

The strong consequence of this theorem is that, for any good subdivision algorithm, one of the subsubdominant eigenvalues must correspond to the zero Fourier block of the subdivision matrix. Otherwise, the resulting surfaces will locally intersect the tangent plane at the extraordinary vertex for almost all initial data. For example, the standard Catmull–Clark algorithm reveals this shortcoming for $n \geq 5$: the Fourier index of μ is $\{2, n-2\}$ and the generated subdivision surfaces are, for generic data, not elliptic in sign. In particular, *they are not convex*.

The second approach to a classification of the central point makes use of the fact that the Gaussian curvature is well defined for all rings $\mathbf{x}^m$ with sufficiently large index m.

Definition 7.11 (Limit-type). Wherever it is well defined, denote by κ_G the Gaussian curvature of a subdivision surface $\mathbf{x}$. The central point $\mathbf{x}^c$ is called

- *elliptic in the limit* if $\kappa_\mathrm{G} > 0$ in a sufficiently small neighborhood of $\mathbf{x}^c$;
- *hyperbolic in the limit* if $\kappa_\mathrm{G} < 0$ in a sufficiently small neighborhood of $\mathbf{x}^c$;
- *hybrid*, if κ_G changes sign in every neighborhood of $\mathbf{x}^c$.

Again, the limit-type of an extraordinary vertex is closely related to the central ring.

Theorem 7.12 (Central surface and limit-type). *Denote by* $\overline{\kappa}_\mathrm{G}$ *the Gaussian curvature of the central ring* $\overline{\mathbf{r}}$. *For generic initial data, the central point is*

- *elliptic in the limit, if* $\overline{\kappa}_\mathrm{G} > 0$;
- *hyperbolic in the limit, if* $\overline{\kappa}_\mathrm{G} < 0$;
- *hybrid, if* $\overline{\kappa}_\mathrm{G}$ *changes sign.*

The proof follows immediately from (7.19/131). Again, this expansion implies more than is stated in the theorem. We see that the sign map of the Gaussian curvature

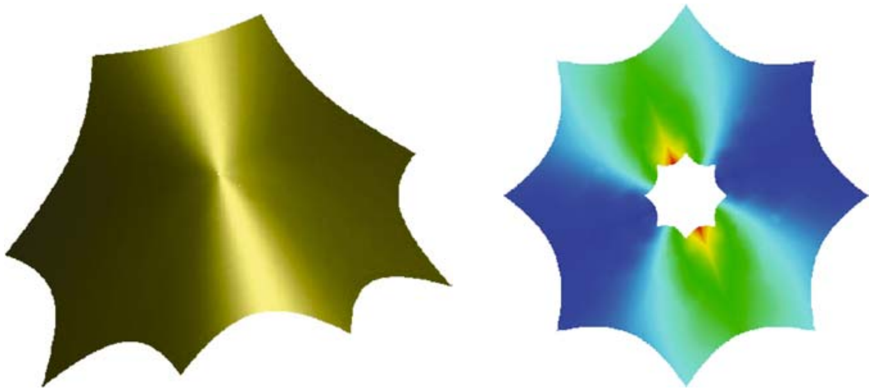

Fig. 7.2 Illustration of hybrid case: Hybrid shape of a subdivision surface generated by a modified Catmull–Clark algorithm. (*left*) Lighted surface with an undesired pinch-off near the central point. (*right*) Part of the surface shaded by Gaussian curvature. *Blue* and *green* colors indicate hyperbolic points, *yellow* and *red* colors indicate elliptic points.

of $\bar{\mathbf{r}}$ is equivalent to that of the rings in an asymptotic way. Thus, the distribution of the sign of the Gaussian curvature in a vicinity of an extraordinary vertex can be studied with the help of the central ring – except at parameters corresponding to parabolic points of the central ring. The study of the Gaussian curvature of the central surface is a basic tool for judging the quality of a subdivision surface since, in applications, fairness requires that the extraordinary point be either elliptic or hyperbolic in sign. The hybrid case leads to shape artifacts (see Fig. 7.2/137). A high quality subdivision algorithm should therefore exclude the hybrid case completely, while facilitating both elliptic and hyperbolic shape in the limit-sense. This is a very strong requirement that is hard to fulfill in practice. To explain the problem, let us consider two sets of initial data: $\mathbf{Q}[0]$ is chosen so that the central ring has positive Gaussian curvature and $\mathbf{Q}[1]$ so that the central ring has negative Gaussian curvature. Now, we consider any continuous transition $\mathbf{Q}[t], t \in [0,1]$, connecting the two cases. The Gaussian curvature of the corresponding central rings is a family $\bar{\kappa}_{\mathrm{G}}[t]$ of functions connecting $\bar{\kappa}_{\mathrm{G}}[0] > 0$ and $\bar{\kappa}_{\mathrm{G}}[1] < 0$. If hybrid behavior is to be excluded then the transition between the positive and the negative case has to be restricted to isolated t-values where $\bar{\kappa}_{\mathrm{G}}[t] \equiv 0$. However, to devise an algorithm with such a property is challenging since the relation between initial data and curvature of the central ring is highly non-linear.

Relating $\bar{\kappa}_{\mathrm{G}}$ to spectral properties is rather difficult and does not promise results beyond Theorem 7.10/136. Since we want to be able to distinguish the desired cup- and saddle-shapes from unstructured local oscillations, we consider a third approach. As we will show in Theorem 7.16/143 of the next section, the subdivision surface $\mathbf{x}$ is C_2^k if and only if the function $\bar{z}$ is a quadratic polynomial in the subdominant eigenrings f_1, f_2, i.e., there exists a constant symmetric (2×2)-matrix H such that the components of the central ring satisfy

$$\bar{\boldsymbol{\xi}} H \cdot \bar{\boldsymbol{\xi}} - \bar{z} = 0.$$

Then, the Gaussian curvature of the central point is given by $\det(H/2)$. In general, no matrix will satisfy the above identity exactly. But one can still try to determine a best approximation in the least squares sense. To this end, we define an inner product for real-valued rings by

$$\langle f, g\rangle := \sum_{j\in\mathbb{Z}_n} \int_{\boldsymbol{\Sigma}^0} f(s,t,j)g(s,t,j)\,dsdt$$

and denote the corresponding norm by $|\cdot|$. Now, for given $\overline{\boldsymbol{\xi}}$ and $\overline{z}$, we define H as the minimizer of the functional

$$\varphi(H) := \left|\overline{\boldsymbol{\xi}}H\cdot\overline{\boldsymbol{\xi}} - \overline{z}\right|^2.$$

The matrix H provides information on the global shape of the central ring in the sense of averaging, and its determinant is now used to define a third notion of hyperbolicity and ellipticity.

Definition 7.13 (Average-type). The central point $\mathbf{x}^{\mathrm{c}}$ is called

- *elliptic in average*, if $\det H > 0$;
- *hyperbolic in average*, if $\det H < 0$.

The average-type is closely related to the Fourier index of the subsubdominant eigenvalue.

Theorem 7.14 (Central surface and average-type). *For generic initial data, the central point is*

- *not elliptic in average unless* $0 \in \mathcal{F}(\mu)$;
- *not hyperbolic in average unless* $\{2, n-2\} \subset \mathcal{F}(\mu)$.

Proof. We start with a simple observation for periodic functions. Let f be $\mathcal{P}$-periodic and g be $\mathcal{Q}$-periodic. By (7.20/135),

$$\langle f, g\rangle = 0 \qquad \text{if} \qquad 0 \notin \mathcal{P} \pm \mathcal{Q}, \tag{7.21}$$

where we recall that $\mathcal{P} \pm \mathcal{Q}$ contains all sums and differences of elements of $\mathcal{P}$ and $\mathcal{Q}$ modulo n. To put the optimization problem in a more convenient form, we set $p := \psi_1^2 + \psi_2^2,\ q := \psi_1^2 - \psi_2^2,\ r := 2\psi_1\psi_2$, and write

$$\varphi(H) = |\boldsymbol{\psi}(LH\cdot L)\cdot\boldsymbol{\psi} - \overline{z}|^2 = |ap + bq + cr - \overline{z}|^2 \tag{7.22}$$

where the coefficients a, b, c are defined by

$$LH\cdot L =: \begin{bmatrix} a+b & c \\ c & a-b \end{bmatrix}. \tag{7.23}$$

The sign of the determinant of H, which we are going to determine, is given by

$$\operatorname{sign}(\det H) = \operatorname{sign}(\det LH\cdot L) = \operatorname{sign}(a^2 - b^2 - c^2).$$

Minimizing the functional φ according to (7.22/138) is equivalent to solving the Gramian system

$$\begin{bmatrix} \langle p,p\rangle & \langle p,q\rangle & \langle p,r\rangle \\ \langle p,q\rangle & \langle q,q\rangle & \langle q,r\rangle \\ \langle p,r\rangle & \langle q,r\rangle & \langle r,r\rangle \end{bmatrix} \begin{bmatrix} a \\ b \\ c \end{bmatrix} = \begin{bmatrix} \langle p,\overline{z}\rangle \\ \langle q,\overline{z}\rangle \\ \langle r,\overline{z}\rangle \end{bmatrix}. \tag{7.24}$$

Now, we determine the periodicity of the functions p, q, r. With the rotation matrix

$$R := \begin{bmatrix} \cos(2\pi/n) & \sin(2\pi/n) \\ -\sin(2\pi/n) & \cos(2\pi/n) \end{bmatrix}$$

we obtain for the segments

$$\begin{aligned} p_j &= \boldsymbol{\psi}_0 R^j \begin{bmatrix} 1 & 0 \\ 0 & 1 \end{bmatrix} \cdot (\boldsymbol{\psi}_0 R^j) = p_0 \\ q_j &= \boldsymbol{\psi}_0 R^j \begin{bmatrix} 1 & 0 \\ 0 & -1 \end{bmatrix} \cdot (\boldsymbol{\psi}_0 R^j) = \cos(4\pi j/n) q_0 - \sin(4\pi j/n) r_0 \\ r^j &= \boldsymbol{\psi}_0 R^j \begin{bmatrix} 0 & 1 \\ -1 & 0 \end{bmatrix} \cdot (\boldsymbol{\psi}_0 R^j) = \cos(4\pi j/n) q_0 + \sin(4\pi j/n) r_0 \end{aligned}$$

and observe that p is $\{0\}$-periodic, while q and r are $\{2\}$-periodic. Hence, by (7.21/138), the off-diagonal elements of the Gramian matrix in the first row and column vanish, $\langle p,q\rangle = \langle p,r\rangle = 0$. If $0 \notin \mathcal{F}(\mu)$, the function $\overline{z}$ is $\mathcal{P}$-periodic with $0 \notin \mathcal{P}$, and the first entry of the right hand side of (7.24/139) becomes $\langle p,\overline{z}\rangle = 0$. Thus, $a = 0$ and $\operatorname{sign}(\det H) = \operatorname{sign}(-b^2 - c^2) \le 0$. If $\{2, n-2\} \not\subset \mathcal{F}(\mu)$, the function $\overline{z}$ is $\mathcal{P}$-periodic with $\{2, n-2\} \cap \mathcal{P} = \emptyset$, and the second and third entry of the right hand side of (7.24/139) become $\langle q,\overline{z}\rangle = \langle r,\overline{z}\rangle = 0$. Thus, $b = c = 0$ and $\operatorname{sign}(\det H) = \operatorname{sign}(a^2) \ge 0$. □

As a consequence of this theorem, we see that the variety of producible shapes will cover both basic average-types only if the subsubdominant eigenvalue is at least triple with Fourier index $\mathcal{F}(\mu) \supset \{0, 2, n-2\}$. However, it must be emphasized that this spectral property is by no means a sufficient condition for a good subdivision algorithm, but merely a basic requirement.

Deeper insight is provided by the concept of *shape charts*, that classify the space of shapes that can be generated by a subdivision algorithm. Let us consider a subdivision algorithm of type (λ, μ, ℓ) with a triple subsubdominant eigenvalue and Fourier index $\mathcal{F}(\mu) = \{0, 2, n-2\}$. Then the third component of the central ring is

$$\overline{z} = \alpha f_3 + \beta f_4 + \gamma f_5,$$

where the coefficients α, β, γ depend on the initial data. Further, we observe that all three shape types of the central point are invariant with respect to regular linear maps. That is, if $\mathbf{P}$ and $\tilde{\mathbf{P}} = \mathbf{P}M$ are initial data related by an invertible (3×3)-matrix M, then the classifications of the corresponding central points $\mathbf{x}^c$ and $\tilde{\mathbf{x}}^c$ coincide. For that reason, we may assume that the matrix L in (7.23/138) is the identity and that, without loss of generality,

$$\alpha^2 + \beta^2 + \gamma^2 = 1, \quad \gamma \geq 0.$$

This observation implies that we can restrict a basic investigation of possible shapes to the two-parameter family

$$\bar{\mathbf{r}}^{\alpha,\beta} := \left[\boldsymbol{\psi},\, \alpha f_3 + \beta f_4 + \sqrt{1-\alpha^2-\beta^2} f_5\right]$$

of surface rings, where the parameters vary inside the unit circle,

$$(\alpha,\beta) \in \Gamma := \left\{(\alpha,\beta) \in \mathbb{R}^2 : \alpha^2 + \beta^2 \leq 1\right\}.$$

A *shape chart* $c := \Gamma \to \mathbb{Z}$ is a map which assigns to each α, β an indicator for the shape-type, for instance

$$c_{\text{limit}}(\alpha,\beta) := \begin{cases} 1 & \text{if } \bar{\kappa}_{\mathrm{G}}^{\alpha,\beta} \geq 0 \\ 0 & \text{if } \bar{\kappa}_{\mathrm{G}}^{\alpha,\beta} \text{ changes sign} \\ -1 & \text{if } \bar{\kappa}_{\mathrm{G}}^{\alpha,\beta} \leq 0, \end{cases} \tag{7.25}$$

where $\bar{\kappa}_{\mathrm{G}}^{\alpha,\beta}$ is the Gaussian curvature of $\bar{\mathbf{r}}^{\alpha,\beta}$. By Theorem 7.12/136, the value c_{limit} (α,β) indicates whether the corresponding subdivision surface is elliptic, hybrid, or hyperbolic in the limit. A shape chart thus summarizes, in a single image for all input data, information about the possible shape in a neighborhood of the central point. In particular, the hybrid region, i.e., the set of pairs (α,β) such that $c_{\text{limit}}(\alpha,\beta) = 0$, can be used to assess the quality of a subdivision algorithm: the smaller that region, the better the algorithm.

Shape charts can be visualized by coloring the different regions of Γ and thereby partitioning the unit circle into two or three subsets as in Fig. 7.3/141. When computing shape charts, possible symmetry properties can be exploited to increase efficiency. Variants on the concept include in particular the following:

- Different normalizations of the triple (α,β,γ). For example, $\max\{|\alpha|, |\beta|, |\gamma|\} = 1$ leads to square-shaped plots.
- Continuous variation of values. For example, the variance of $\operatorname{trace} W$, see (7.16/131), shows the deviation of the mean curvature of the rings $\mathbf{x}^m$ from a constant value.

7.3 Conditions for C_2^k-Algorithms

In this section, we derive necessary and sufficient conditions for curvature continuity at the central point. It turns out that the sufficient conditions are extremely restrictive. This explains the failure of many early attempts to construct such algorithms. We start with a necessary condition on the spectrum of the subdivision matrix.

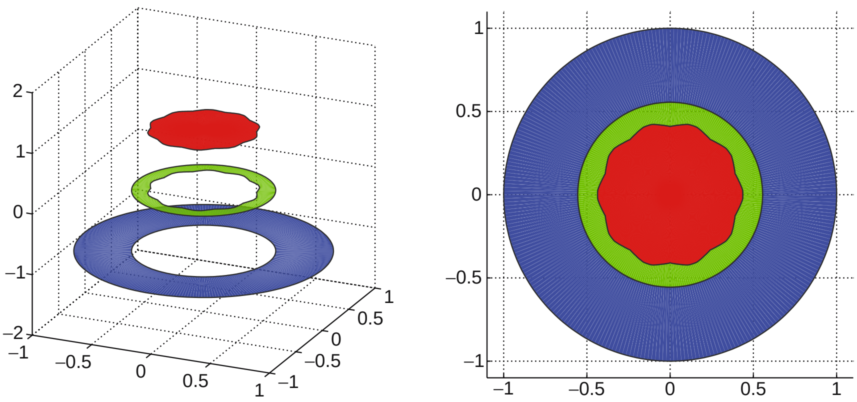

Fig. 7.3 Illustration of (7.25/140): Shape chart for the Catmull–Clark algorithm with $n = 10$ and flexible weights. (*left*) *Perspective view* and (*right*) *top view*. Respectively, the colors *red*, *green*, and *blue* indicate elliptic, hybrid, and hyperbolic behavior in the limit.

Theorem 7.15 (Necessity of $\mu \leq \lambda^2$). *A subdivision algorithm of type* (λ, μ, ℓ) *can be* C_2^k *only if* $(\mu, \ell) \preccurlyeq (\lambda^2, 0)$.

Proof. Let us recall the expansion (7.14/130),

$$\mathbf{W}^m \stackrel{*}{=} \varrho^{m,\ell} \, (\mathbf{T}^{\mathrm{c}})^{\mathrm{t}} \, W \mathbf{T}^{\mathrm{c}}, \quad \varrho = \frac{\mu}{\lambda^2}.$$

In view of Lemma 7.5/132, which states that $W \neq 0$ for generic initial data, we see that pointwise convergence of the sequence $\mathbf{W}^m$, as required by Theorem 2.14/28, is possible only if $\varrho^{m,\ell}$ converges. □

If $\mu < \lambda^2$ then $\varrho < 1$ and $\mathbf{W}^m$ converges to 0. According to Theorem 2.14/28, this guarantees curvature continuity. However, in this case the central point is necessarily a *flat spot*, i.e., the principal curvatures vanish here. For most applications, such a restriction is not acceptable so that we do not elaborate on that case. Rather, we seek conditions for *nontrivial curvature continuity* and assume from now on

$$(\mu, \ell) = (\lambda^2, 0).$$

Then, according to Theorem 2.14/28, a necessary and sufficient condition for curvature continuity is that the limit

$$\mathbf{W}^{\mathrm{c}} := \lim_{m \to \infty} \mathbf{W}^m = \begin{bmatrix} W & 0 \\ 0 & 0 \end{bmatrix}$$

be a constant (3×3)-matrix, i.e., it does not depend on the arguments (s, t, j). Now, we *reparametrize* the rings $\mathbf{x}^m$ via the inverse of the planar ring $\overline{\boldsymbol{\xi}} = \psi L$, which is an embedding for generic data,

$$\tilde{\mathbf{x}}^m(u, v) := \mathbf{x}^m(\mathbf{s}), \quad \mathbf{s} := \overline{\boldsymbol{\xi}}^{-1}(u, v) \in \mathbf{S}_n^0.$$

By (2.5/22), the corresponding embedded Weingarten maps are equal up to sign:

$$\tilde{\mathbf{W}}^m(u,v) = \pm\mathbf{W}^m(\mathbf{s}).$$

Following (7.6/128), the asymptotic expansion of $\tilde{\mathbf{x}}^m$ is

$$(\tilde{\mathbf{x}}^m - \mathbf{x}^{\mathrm{c}})\cdot\mathbf{F}^{\mathrm{c}} \stackrel{*}{=} \big[\lambda^m u, \lambda^m v, \lambda^{2m}\tilde{z}(u,v)\big],$$

where $\tilde{z}(u,v) := \overline{z}(\mathbf{s})$. Some elementary computations now yield

$$D\tilde{\mathbf{x}}^m \stackrel{*}{=} \lambda^m\mathbf{T}^{\mathrm{c}},\quad (D\tilde{\mathbf{x}}^m)^+ \stackrel{*}{=} \lambda^{-m}(\mathbf{T}^{\mathrm{c}})^{\mathrm{t}},\quad \tilde{\mathbf{n}}^m \stackrel{*}{=} \mathbf{n}^{\mathrm{c}},\quad \tilde{I\!I}^m \stackrel{*}{=} \lambda^{2m}\begin{bmatrix}\tilde{z}_{uu} & \tilde{z}_{uv}\\ \tilde{z}_{uv} & \tilde{z}_{vv}\end{bmatrix}$$

so that

$$\tilde{\mathbf{W}}^m \stackrel{*}{=} (\mathbf{T}^{\mathrm{c}})^{\mathrm{t}}\tilde{W}\mathbf{T}^{\mathrm{c}},\quad \tilde{W} := \begin{bmatrix}\tilde{z}_{uu} & \tilde{z}_{uv}\\ \tilde{z}_{uv} & \tilde{z}_{vv}\end{bmatrix}.$$

Hence, the limit $\tilde{\mathbf{W}}^{\mathrm{c}} = \pm\mathbf{W}^{\mathrm{c}}$ is constant if and only if the three functions $\tilde{z}_{uu}, \tilde{z}_{uv}$, and $\tilde{z}_{vv}$ are constant. This holds if and only if

$$\tilde{z} \in \operatorname{span}\big\{1, u, v, u^2, uv, v^2\big\}.$$

That is, $\tilde{z}$ is a quadratic polynomial in u, v. Since $[u,v] = \overline{\boldsymbol{\xi}}(\mathbf{s})$, and the components of $\overline{\boldsymbol{\xi}}$ are linear combinations of the subdominant eigenrings f_1 and f_2, we obtain the equivalent condition

$$\overline{z} \in \operatorname{span}\big\{1, f_1, f_2, f_1^2, f_1 f_2, f_2^2\big\}.$$

Now, we consider the central spline $\mathbf{x}$ according to Definition 7.2/128. As observed above, its rings satisfy

$$\bar{\mathbf{x}}^0 = \bar{\mathbf{r}} = \big[\overline{\boldsymbol{\xi}}, \overline{z}\big],\quad \bar{\mathbf{x}}^m = \big[\lambda^m\overline{\boldsymbol{\xi}}, \lambda^{2m}\overline{z}\big].$$

We know that $\overline{z}$ is a quadratic polynomial in the components of $\overline{\boldsymbol{\xi}}$ and write $\overline{z} = p(\overline{\boldsymbol{\xi}})$. Being scaled copies of $\bar{\mathbf{x}}^0$, the other rings satisfy similar equations $\lambda^{2m}\overline{z} = p^m(\lambda^m\overline{\boldsymbol{\xi}})$, where the functions $p^m := \lambda^{2m}p(\lambda^{-m}\cdot)$ are also quadratic polynomials. However, because the rings $\bar{\mathbf{x}}^m$ join C^2, all these polynomials must in fact coincide, i.e., $p^m = p$. The resulting relation

$$\lambda^{2m}p = p(\lambda^m\cdot),\quad m \in \mathbb{N}_0,$$

shows that p is a *homogeneous* quadratic polynomial. Hence,

$$\overline{z} \in \operatorname{span}\big\{f_1^2, f_1 f_2, f_2^2\big\}.$$

Finally, because

$$\overline{z} = \sum_{q=3}^{\bar{q}} f_q\mathbf{p}_q\cdot\mathbf{n}^{\mathrm{c}} = a_1 f_1^2 + a_2 f_1 f_2 + a_3 f_2^2 \tag{7.26}$$

must hold for any choice of generic initial data, we obtain the following result.

Theorem 7.16 (C_2^k-criterion). *A subdivision algorithm of type $(\lambda, \lambda^2, 0)$ is a C_2^k-algorithm if and only if the subsubdominant eigenrings satisfy*

$$f_q \in \operatorname{span}\{f_1^2, f_1 f_2, f_2^2\}, \quad q = 3, \ldots, \bar{q}.$$

Moreover, $\bar{q} \leq 5$

Proof. The first part of the theorem was derived above. The second part, saying that the subsubdominant eigenvalue is at most triple, follows from linear independence of the subsubdominant eigenrings according to Lemma 4.22/78. □

The functional dependence required by the theorem is extremely restrictive and accounts, for instance, for the impossibility of finding C_2^2-variants on the Catmull–Clark algorithm. To see this, we now focus on piecewise polynomial algorithms.

Definition 7.17 ($C_r^{k,q}$-algorithm). Let $\{\boldsymbol{\Sigma}_i\}_i$ be a finite family of intervals forming a partition of the domain $\boldsymbol{\Sigma}^0$ of segments,

$$\boldsymbol{\Sigma}^0 = \bigcup_i \boldsymbol{\Sigma}_i.$$

A ring $\mathbf{x}^m \in C^k(\mathbf{S}_n^0, \mathbb{R}^d, G)$ is said to have *bi-degree* q *with respect to* $\{\boldsymbol{\Sigma}_i\}_i$ if $\mathbf{x}^m$ restricted to $\boldsymbol{\Sigma}_i$ is a polynomial of bi-degree at most q for all i, and a polynomial of bi-degree q for at least one i; we write

$$\deg \mathbf{x}^m = q.$$

Further, a C_r^k-subdivision algorithm (A, G) is called a $C_r^{k,q}$*-algorithm*, if

$$\max_\ell \deg g_\ell = q$$

for the generating rings g_ℓ.

For instance, the Catmull–Clark algorithm is a $C_1^{2,3}$-algorithm, and the Doo–Sabin algorithm is a $C_1^{1,2}$-algorithm. For tensor-product splines with simple knots, the bi-degree q exceeds the smoothness k only by 1. However, non-trivial $C_2^{k,q}$-algorithms require a substantially higher degree. The results in that direction are all based on the following observation:

Lemma 7.18 (Degree estimate for ψ). *For $n \neq 4$, the characteristic map ψ of a standard $C_1^{k,q}$-algorithm satisfies*

$$\deg \boldsymbol{\psi} > k.$$

Proof. Let us assume that $\deg \boldsymbol{\psi} \leq k$. Then the segments $\boldsymbol{\psi}_j$ are in fact not piecewise polynomials on a partition, but simply polynomials on $\boldsymbol{\Sigma}^0$. Equally, two neighboring segments $\boldsymbol{\psi}_j$ and $\boldsymbol{\psi}_{j+1}$ differ only by a change of parameters,

$$\boldsymbol{\psi}_{j+1}(s,t) = \boldsymbol{\psi}_j(t, -s).$$

Hence, $\boldsymbol{\psi}_{j+4} = \boldsymbol{\psi}_j$, implying that injectivity is possible only for $n = 4$. □

For $n = 4$, the characteristic ring of the Catmull–Clark-algorithm and of the Doo–Sabin-algorithm have $\deg \boldsymbol{\psi} = 1$. For $n \neq 4$, the lemma and Theorem 7.16/143 suggest, and the following shows, that the generating system G must have at least bi-degree $2k + 2$ to represent subsubdominant eigenfunctions.

Theorem 7.19 (Degree estimate for $C_2^{k,q}$-algorithms). *Let $n \neq 4$. For a non-trivial $C_2^{k,q}$-algorithm with characteristic ring $\boldsymbol{\psi}$,*

$$q \geq 2 \deg \boldsymbol{\psi} \geq 2k + 2.$$

In particular, the lowest degree for $k = 2$ is $q = 6$.

Proof. By (7.26/142), with the complex characteristic ring$f = f_1 + \mathbf{i} f_2$, the j-th segment of the normal component of the central ring can be written as

$$\begin{aligned} \bar{z}_j &= a_1 f_{1,j}^2 + a_2 f_{1,j} f_{2,j} + a_3 f_{2,j}^2 \\ &= \operatorname{Re}(\alpha f_j^2) + \beta |f_j|^2 = \operatorname{Re}(\alpha w_n^{2j} f_0^2) + \beta |f_0|^2, \end{aligned}$$

where $\alpha := (a_1 - a_3 - \mathbf{i} a_2)/2, \beta := (a_1 + a_3)/2$. The last equality follows from (5.21/103), saying that the segments of f are related by $f_j = w_n^j f_0$. By Lemma 7.18/143, the complex-valued piecewise polynomial f_0 has degree $\deg f_0 \geq k + 1$.

For a bivariate polynomial p of degree $d := \deg p$ we define the leading coefficient $c[p] \neq 0$ and the leading monomial $m[p](s,t) = s^\ell t^{d-\ell}$ by the split

$$p = c[p]\, m[p] + T[p],$$

where the trailing term

$$T[p] := \sum_{i=\ell+1}^{d} c_i s^i t^{d-\ell} + \sum_{i+k<d} c_{i,k} s^i t^k$$

summarizes all terms of degree d which contain at least the factor $s^{\ell+1}$, and all terms of degree $< d$. Obviously, for two polynomials p_1, p_2 with $m[p_1] = m[p_2]$ it is

$$c[p_1 p_2] = c[p_1]\, c[p_2], \quad m[p_1 p_2] = (m[p_1])^2.$$

When restricted to a suitable subset of its domain,

$$f_0 = c[f_0] m[f_0] + T[f_0], \quad \deg m[f_0] \geq k + 1.$$

Because the characteristic ring f can be scaled arbitrarily, we may assume without loss of generality that the leading coefficient is $c[f_0] = 1$. Hence,

$$f_0^2 = (m[f_0])^2 + T\big[f_0^2\big], \quad |f_0|^2 = f_0 \overline{f_0} = (m[f_0])^2 + T\big[|f_0^2|\big],$$

and the coefficient of $\overline{z}_j$ to the monomial $(m[f_0])^2$ is

$$\mathrm{Re}(\alpha w_n^{2j}) + \beta.$$

This expression can vanish for all $j \in \mathbb{Z}_n$ only if $\alpha = \beta = 0$. This implies $a_1 = a_2 = a_3 = 0$ and $\overline{z} = 0$, contradicting the assumption that the initial data be generic. Hence, $m[\overline{z}_j] = (m[f_0])^2$ at least for one j, showing that the degree of $\bar{z}$ is bounded by $\deg \overline{z} \geq \deg \overline{z}_j = 2d[f_0] \geq 2(k+1)$. □

7.4 A Framework for C_2^k-Algorithms

In this section, we provide a framework for constructing C_2^k-algorithms. So far, the algorithm (A, G) was assumed to be given, and $\boldsymbol{\psi}$ was determined as the planar ring corresponding to the subdominant eigenvalues of the subdivision matrix A. By contrast, we now start with a function $\boldsymbol{\varphi} \in C^k(\mathbf{S}_n^0, \mathbb{R}^2, G)$ and then derive a matrix A so that (A, G) defines a C_2^k-algorithm with $\boldsymbol{\psi} := \boldsymbol{\varphi}$ as its characteristic ring. More precisely, we say that the planar ring $\boldsymbol{\varphi} \in C^k(\mathbf{S}_n^0, \mathbb{R}^2, G)$ is a *regular C^k-embedding of $\mathbf{S}_n^0$ with scale factor* λ if it has the two key properties of a characteristic ring, i.e.,

- $\boldsymbol{\varphi}$ is regular and injective, and
- there exists a real number $\lambda \in (0, 1)$ such that $\boldsymbol{\varphi}$ and $\lambda\boldsymbol{\varphi}$ join C^2 according to (4.8/62) when regarded as consecutive rings.

For instance, the characteristic ring of the Catmull–Clark algorithm represents a regular C^2-embedding of bi-degree 3, which may be used to construct a $C_2^{2,6}$-algorithm. But as mentioned already above, there is no need to derive $\boldsymbol{\varphi}$ from an existing algorithm. The image of $\boldsymbol{\varphi}$ is denoted by

$$\boldsymbol{\Omega} := \boldsymbol{\varphi}(\mathbf{S}_n^0).$$

Now, we define a family of reparametrization operators, taking rings to functions on scaled copies of $\boldsymbol{\Omega}$.

Definition 7.20 (Reparametrization $\mathcal{R}_m$). For $m \in \mathbb{N}_0$, the *reparametrization operator* $\mathcal{R}_m$ maps a ring $\mathbf{p} \in C^k(\mathbf{S}_n^0, \mathbb{R}^d)$ to a C^k-function $\mathbf{q} := \mathcal{R}_m[\mathbf{p}]$ on $\lambda^m \boldsymbol{\Omega} \subset \mathbb{R}^2$,

$$\mathbf{q} : \lambda^m \boldsymbol{\Omega} \ni \boldsymbol{\xi} \mapsto \mathbf{p}(\boldsymbol{\varphi}^{-1}(\lambda^{-m}\boldsymbol{\xi})) \in \mathbb{R}^d.$$

The inverse operator $\mathcal{R}_m^{-1}$ maps a C^k-function $\mathbf{q}$ on $\lambda^m \boldsymbol{\Omega}$ to a ring $\mathbf{p} := \mathcal{R}_m^{-1}[\mathbf{q}] \in C^k(\mathbf{S}_n^0, \mathbb{R}^d)$,

$$\mathbf{p} : \mathbf{S}_n^0 \ni \mathbf{s} \mapsto \mathbf{q}(\lambda^m \boldsymbol{\varphi}(\mathbf{s})).$$

The operator $\mathcal{R}_m$, and equally $\mathcal{R}_m^{-1}$, is linear in the sense that $\mathcal{R}_m[\alpha f + \beta g] = \alpha\mathcal{R}_m[f] + \beta\mathcal{R}_m[g]$. Given $\boldsymbol{\varphi}$, we denote the space of bivariate polynomials of total degree 2 restricted to $\lambda^m \boldsymbol{\Omega}$ by $\mathbb{P}_2(\lambda^m \boldsymbol{\Omega})$. The following definition is crucial. It characterizes subdivision algorithms which are able to represent rings corresponding to quadratic polynomials, and generate such quadratic rings from quadratic rings.

Definition 7.21 (Quadratic precision). The subdivision algorithm (A,G) has *quadratic precision* with respect to $\boldsymbol{\varphi}$ if

- for each quadratic polynomial $p \in \mathbb{P}_2(\boldsymbol{\Omega})$ there exists a real-valued ring $\mathbf{x}^0 \in C^k(\mathbf{S}_n^0, \mathbb{R}, G)$ with
$$\mathcal{R}_0[\mathbf{x}^0] = p,$$
- for consecutive rings $\mathbf{x}^0 = G\mathbf{Q}$ and $\mathbf{x}^1 = GA\mathbf{Q}$,
$$\mathcal{R}_0[\mathbf{x}^0] \in \mathbb{P}_2(\boldsymbol{\Omega}) \quad \text{implies} \quad \mathcal{R}_0[\mathbf{x}^1] \in \mathbb{P}_2(\boldsymbol{\Omega}).$$

First, we observe that for a subdivision algorithm (A,G) with quadratic precision, $\mathcal{R}_0[\mathbf{x}^0] \in \mathbb{P}_2(\boldsymbol{\Omega})$ implies $\mathcal{R}_0[\mathbf{x}^m] \in \mathbb{P}_2(\boldsymbol{\Omega})$ and also $\mathcal{R}_m[\mathbf{x}^m] \in \mathbb{P}_2(\lambda^m\boldsymbol{\Omega})$ for all m. Second, we consider the sequence

$$\mathcal{R}_0[\mathbf{x}^0],\ \mathcal{R}_1[\mathbf{x}^1],\ \mathcal{R}_2[\mathbf{x}^2],\ \ldots,$$

starting from $\mathcal{R}_0[\mathbf{x}^0] \in \mathbb{P}_2(\boldsymbol{\Omega})$. Corresponding to consecutive rings that join C^2, all these polynomials coincide in the sense that they must have the same monomial expansion. However, strictly speaking, they are not equal because the domains are different. To account for that fact, we write

$$\mathcal{R}_0[\mathbf{x}^0] \cong \mathcal{R}_m[\mathbf{x}^m], \quad m \in \mathbb{N}.$$

In particular, if $\mathcal{R}_0[\mathbf{x}^0]$ is a monomial of total degree $\ell \le 2$, we have

$$\mathcal{R}_0[\mathbf{x}^m] = \lambda^{\ell m}\mathcal{R}_0[\mathbf{x}^0]. \tag{7.27}$$

Remarkably, quadratic precision immediately yields an appropriate eigenstructure for (A,G).

Lemma 7.22 (Quadratic precision yields correct spectrum). *Let $\boldsymbol{\varphi}$ be a regular C^k-embedding of $\mathbf{S}_n^0$ with scale factor λ. If (A,G) has quadratic precision with respect to $\boldsymbol{\varphi}$, then there exist eigenvalues λ_i, eigenvectors v_i, and eigenrings $f_i := Gv_i$, satisfying*

$$\lambda_0 = 1, \quad \lambda_1 = \lambda_2 = \lambda, \quad \lambda_3 = \lambda_4 = \lambda_5 = \lambda^2,$$
$$f_0 = 1, \quad [f_1, f_2] = \boldsymbol{\varphi}, \quad f_3 = f_1^2,\ f_4 = f_1 f_2,\ f_5 = f_2^2.$$

Here, with a slight abuse of notation, we indexed eigenvalues without assuming that the whole sequence is ordered by modulus. In particular, further eigenvalues with modulus greater than λ^2 are not excluded a priori.

Proof. With $\boldsymbol{\xi} = (x,y)$, we define the monomials

$$p_0(\boldsymbol{\xi}) = 1,\ p_1(\boldsymbol{\xi}) = x,\ p_2(\boldsymbol{\xi}) = y,\ p_3(\boldsymbol{\xi}) = x^2,\ p_4(\boldsymbol{\xi}) = xy,\ p_5(\boldsymbol{\xi}) = y^2$$

in $\mathbb{P}_2(\boldsymbol{\Omega})$. For $i = 0,\ldots,5$, we have $\lambda_i = \lambda^{\ell_i}$, where ℓ_i is the total degree of p_i. By definition of quadratic precision, the function $f_i := \mathcal{R}_0^{-1}[p_i] = p_i \circ \boldsymbol{\varphi}$ can be written as $f_i = Gv_i'$ for some vector $v_i' \neq 0$. By (7.27/146), $\mathcal{R}_0[GA^m v_i'] = \lambda^{\ell_i m} p_i$, and hence, applying $\mathcal{R}_0^{-1}$ on both sides,

$$GA^m v_i' = \lambda_i^m f_i = \lambda_i^m G v_i'.$$

If G is linearly independent, it follows immediately that v_i' is an eigenvector of A to λ_i, but we have to show that the same is true in general.

For $k \in \mathbb{N}_0$, let $v_i := \lambda_i^{-k} A^k v_i'$. Then

$$Gv_i = \lambda_i^{-k} GA^k v_i' = f_i$$

shows that v_i is another possible choice of coefficients corresponding to the polynomial p_i. As before,

$$GA^m v_i = \lambda_i^m f_i = \lambda_i^m G v_i. \tag{7.28}$$

With $A = VJV^{-1}$ the Jordan decomposition of A, let

$$w' := V^{-1} v_i', \quad w := V^{-1} v_i = \lambda_i^{-k} J^k w'.$$

Recalling (4.25/74), F and w are partitioned into blocks F_r and w_r corresponding to the Jordan blocks J_r of J. Condition (7.28/147) yields the equivalent system

$$F_r J_r^m w_r = \lambda_i^m F_r w_r, \quad r = 0, \ldots, \bar{r}.$$

When determining solutions w_r, we distinguish two cases: First, if the eigenvalue corresponding to J_r is $\lambda_r = 0$, then $w_r = \lambda_i^{-k} J_r^k w_r' = 0$ is the only solution for k chosen sufficiently large.

Second, if $\lambda_r \neq 0$, then Lemma 4.22/78 guarantees that the eigenfunction f_r^0 does not vanish. Of course, the trivial solution $w_r = 0$ is possible. Otherwise, if $w_r \neq 0$, let ν denote the largest index of a non-vanishing component, i.e., $w_r^i = 0$ for $i > \nu$ and $w_r^\nu \neq 0$. By (4.27/74), we have the asymptotic expansion

$$\lambda_i^m F_r w_r = F_r J_r^m w_r \stackrel{*}{=} \lambda_r^{m,\nu} f_r^0 w_r^\nu,$$

implying $\lambda_i = \lambda_r$ and $\nu = 0$. Hence, $w_r = [w_r^0; 0; \ldots; 0]$ is an eigenvector of J_r to the eigenvalue λ_i. Summarizing, we have $J_r w_r = \lambda_i w_r$ for all r. Therefore, $Jw = \lambda_i w$ and $Av_i = \lambda_i v_i$.

For $i = 0, \ldots, 5$, we obtain the eigenvalues $\lambda_0 = 1, \lambda_1 = \lambda_2 = \lambda$ and $\lambda_3 = \lambda_4 = \lambda_5 = \lambda^2$, as stated. The corresponding dominant and subdominant eigenrings are $f_0 = 1$, and $[f_1, f_2] = \boldsymbol{\varphi}$. Hence, $f_3 = p_3 \circ \boldsymbol{\varphi} = p_1^2 \circ \boldsymbol{\varphi} = (p_1 \circ \boldsymbol{\varphi})^2 = f_1^2$, and equally $f_4 = f_1 f_2,\ f_5 = f_2^2$. □

Together, Lemma 7.22/146 and Theorem 7.16/143 show that quadratic precision and scalable embeddings yield promising candidates for C^k_2-algorithms.

Theorem 7.23 (Quadratic precision suggests C^k_2-algorithm). *Let $\boldsymbol{\varphi}$ be a regular C^k-embedding of $\mathbf{S}_n^0$ with scale factor λ. If the symmetric C^k-subdivision algorithm (A, G) has quadratic precision with respect to $\boldsymbol{\varphi}$, and if $|\lambda_i| < \lambda^2$ for all $i > 5$, then (A, G) is of type $(\lambda, \lambda^2, 0)$ and defines a C^k_2-algorithm.*

Now, we describe a four-step procedure which yields subdivision algorithms with quadratic precision. The four steps *reparametrization – extension – turn-back – projection* suggest the acronym *PTER* for the framework, where as usual the concatenation of operators is from right to left.

Let us assume that a C^k-system G of generating rings and a regular C^k-embedding $\boldsymbol{\varphi}$ with scale factor λ are given and have the following properties:

- The generating rings g_ℓ are piecewise polynomial with maximal degree q in the sense of Definition 7.17/143.
- In view of Theorem 7.19/144, the embedding $\boldsymbol{\varphi} = G[v_1, v_2]$ has degree $\deg \boldsymbol{\varphi} \leq k/2$.
- There exist vectors v_3, v_4, v_5 with

$$Gv_3 = (Gv_1)^2, \quad Gv_4 = (Gv_1)(Gv_2), \quad Gv_5 = (Gv_2)^2$$

  to account for Theorem 7.16/143. In particular, this assumption is fulfilled if G spans the space of *all* piecewise polynomials with respect to the given partition and the given order of continuity.

To simplify notation, we describe how to compute $\mathbf{x}^1 = G\mathbf{Q}^1$ from $\mathbf{x}^0 = G\mathbf{Q}$ for given initial data $\mathbf{Q}$. But the whole procedure is linear and independent of the level m so that it defines a stationary algorithm. The building blocks are characterized as follows:

R – *Reparametrization:* Reparametrize the ring $\mathbf{x}^0$ as a function $\mathbf{y}^0$ on $\boldsymbol{\Omega}$,

$$\mathbf{y}^0 := \mathcal{R}_0[\mathbf{x}^0].$$

E – *Extension:* Extend $\mathbf{y}^0$ to a function $\mathbf{y}^1$ defined on $\lambda\boldsymbol{\Omega}$ such that quadratic polynomials are extended by themselves,

$$\mathbf{y}^0 \cong \mathbf{y}^1 \quad \text{if} \quad \mathbf{y}^0 \in \mathbb{P}_2(\boldsymbol{\Omega}).$$

We note that smooth contact is required only for quadratic polynomials. In general, $\mathbf{y}^0$ and $\mathbf{y}^1$ do not need to join continuously. Since G is not necessarily linear independent, $\mathbf{y}^1$ may depend not only on $\mathbf{y}^0$, but also directly on the initial data $\mathbf{Q}$. We write in terms of the linear *extension operator* $\mathcal{E}$

$$\mathbf{y}^1 := \mathcal{E}[\mathbf{Q}, \mathbf{y}^0].$$

Some examples of $\mathcal{E}$ are as follows:
(i) A projection from the space of functions on $\boldsymbol{\Omega}$ onto some finite dimensional space $\mathbb{P}(\boldsymbol{\Omega})$ of bivariate polynomials containing $\mathbb{P}_2(\boldsymbol{\Omega})$. This projection could be obtained, e.g., by a least squares fit or by an interpolant $\tilde{\mathbf{y}}^0 \in \mathbb{P}(\boldsymbol{\Omega})$ of $\mathbf{y}^0$. Then, the extension is defined by the polynomial $\tilde{\mathbf{y}}^0$, i.e., $\mathbf{y}^1 \cong \tilde{\mathbf{y}}^0$. In the same way, also spaces of piecewise polynomials can be used.
(ii) The minimizer of some positive semi-definite quadratic fairness functional $\mathcal{F}$, acting on functions defined on $\lambda\boldsymbol{\Omega}$, with the property that $\mathcal{F}$ vanishes on $\mathbb{P}_2(\lambda\boldsymbol{\Omega})$. For instance, for functions $\mathbf{y}^1$ joining C^k with $\mathbf{y}^0$, one can consider

$$\mathcal{F}(\mathbf{y}^1) := \int_{\lambda\boldsymbol{\Omega}} \Delta^k \mathbf{y}^1(\boldsymbol{\xi})\, d\boldsymbol{\xi} \to \min$$

or discrete variants thereof. Also here, if $\mathbf{y}^0 \in \mathbb{P}(\boldsymbol{\Omega})$, then $\mathbf{y}^1 \cong \mathbf{y}^0$ because $\mathcal{F}(\mathbf{y}^1) = 0$ for $\mathbf{y}^1 \in \mathbb{P}_2(\lambda\boldsymbol{\Omega})$.

T – *Turn-back:* Convert the function $\mathbf{y}^1$ back into a ring,

$$\tilde{\mathbf{x}}^1 := \mathcal{R}_1^{-1}[\mathbf{y}^1].$$

In general, this ring is neither in the span of G, nor does it join smoothly with $\mathbf{x}^0$.

P – *Projection:* Project $\tilde{\mathbf{x}}^1$ into the subspace of $C^k(\mathbf{S}_n^0, \mathbb{R}^d, G)$ consisting of rings that join C^k with $\mathbf{x}^0$. The coefficients $\mathbf{Q}^1$ of the resulting ring $\mathbf{x}^1 = G\mathbf{Q}^1$ are obtained by a linear operator $\mathcal{P}$,

$$\mathbf{Q}^1 := \mathcal{P}[\mathbf{Q}, \tilde{\mathbf{x}}^1],$$

where the first argument provides information to enforce the C^k-condition. Crucially, $\mathcal{P}$ has to be chosen such that $\mathbf{x}^1 = \tilde{\mathbf{x}}^1$ if $\tilde{\mathbf{x}}^1$ is a quadratic polynomial in the components of $\boldsymbol{\varphi}$, i.e., if $\mathcal{R}_0[\tilde{\mathbf{x}}^1] \in \mathbb{P}_2(\boldsymbol{\Omega})$. Thus, $\mathcal{P}$ is typically defined by a constrained least squares fit with respect to some inner product, either continuous or discrete,

$$\|\tilde{\mathbf{x}}^1 - G\mathbf{Q}^1\| \to \min.$$

We note that, if G is linearly dependent, $\mathcal{P}$ is not uniquely determined by the above optimization problem.

Together, the PTER-framework yields the new coefficients

$$\tilde{A}\mathbf{Q} := \mathbf{Q}^1 := \mathcal{P}[\mathbf{Q}, \mathcal{R}_1^{-1}[\mathcal{E}[\mathbf{Q}, \mathcal{R}_0[G\mathbf{Q}]]]].$$

The columns of $\tilde{A}$ are obtained by substituting in unit vectors for the argument $\mathbf{Q}$. Then, any ineffective eigenvectors should be removed from $\tilde{A}$ according to Theorem 4.20/77 to obtain a genuine subdivision matrix A.

Theorem 7.24 (The PTER-framework works). *The PTER-framework yields a* $C_2^{k,q}$*-algorithm* (A, G) *if* $|\lambda_i| < \lambda^2$ *for* $i > 5$.

Proof. Tracing subdivision of the ring $\mathbf{x}^0$ corresponding to a quadratic function $\mathcal{R}[\mathbf{x}^m]$, one easily sees that the so constructed algorithm (A, G) has quadratic precision and the assumptions of Theorem 7.23/147 are satisfied. □

7.5 Guided Subdivision

The framework in the previous section is inspired by and closely related to that of *Guided subdivision*. Guided subdivision aims at controlling the shape by means of a so-called *guide surfaces*, or guide for short. This guide g serves as an outline of the local shape of the subdivision surface $\mathbf{x}$ to be constructed, and is not changed as subdivision proceeds. The sequence of rings will be defined such that consecutive rings join C^2 and the reparametrization of $\mathbf{x}^m$ approximates the guide on $\lambda^m \boldsymbol{\Omega} = \lambda^m \boldsymbol{\varphi}(\mathbf{S}_n^0)$. For a given regular C^k-embedding $\boldsymbol{\varphi}$ of $\mathbf{S}_n^0$ with scale factor λ, we expect

$$\mathcal{R}_m[\mathbf{x}^m] \approx \mathbf{g}_{|\lambda^m \boldsymbol{\Omega}},$$

or equivalently

$$\mathbf{x}^m \approx \mathcal{R}_m^{-1}[\mathbf{g}].$$

Thus, the shape of the spline surface approximates the shape of the guide.

It is instructive to explain the concept of Guided subdivision by means of a concrete and actually quite simple setting. Just like the framework, it has many options, generalizations and extensions, such as algorithms for triangular patches or for higher smoothness and precision.

Let $\{\boldsymbol{\Sigma}_i\}_{i=1}^3$ be the natural partition of $\boldsymbol{\Sigma}^0$ into three squares with side length $1/2$, and choose smoothness $k = 2$ and bi-degree $q = 7$. Bi-degree 7 is not minimal, but chosen to simplify the exposition of Hermite sampling below.

Due to the partition, for $0 \le \ell \le k = 2$ and all $j \in \mathbb{Z}_n$, the functions

$$D_1^\ell \mathbf{x}^m(1/2, \cdot, j), \quad D_2^\ell \mathbf{x}^m(\cdot, 1/2, j)$$

defining the inner boundary of $\mathbf{x}^m$ are *polynomials* of degree at most q. Hence, the C^2-contact conditions (4.8/62) imply that the corresponding functions

$$D_1^\ell \mathbf{x}^{m+1}(1, \cdot, j), \quad D_2^\ell \mathbf{x}^{m+1}(\cdot, 1, j),$$

at the outer boundary of $\mathbf{x}^{m+1}$ are also not piecewise polynomial but each a single polynomial of degree $q = 7$ or less. Therefore, we define $\tilde{G} = [\tilde{g}_1, \dots, \tilde{g}_{\tilde{q}}]$ to be a system of rings spanning the linear subspace of all C^2-rings with bi-degree $q = 7$, and for which

$$D_1^\ell \tilde{g}_\ell(1, \cdot, j), \quad D_2^\ell \tilde{g}_\ell(\cdot, 1, j), \quad 0 \le \ell \le k = 2,$$

are polynomials of degree ≤ 7. Then a ring in $C^k(\mathbf{S}_n^0, \mathbb{R}^d, \tilde{G})$ is uniquely defined by its partial derivatives up to order $(\frac{q-1}{2}, \frac{q-1}{2}) = (3, 3)$ at the $4n$ points

$$\mathbf{s}_j^1 := (1/2, 0, j),\ \mathbf{s}_j^2 := (1, 0, j),\ \mathbf{s}_j^3 := (1/2, 1/2, j),\ \mathbf{s}_j^4 := (1, 1, j), \quad j \in \mathbb{Z}_n, \tag{7.29}$$

see Fig. 7.4/151. To formalize the construction of rings from partial derivatives, we define the tensor-product *Hermite operator* $\mathcal{H}$ of order $(3, 3)$. The operator $\mathcal{H}$ maps a ring $\mathbf{x}^0$ to the (4×4)-matrix

$$\mathcal{H}[\mathbf{x}^0] := \left[D_1^\alpha D_2^\beta \mathbf{x}^0\right]_{(0,0) \le (\alpha, \beta) \le (3,3)}$$

of partial derivatives up to order $(3, 3)$.

For simplicity, we consider polynomial guides only. To represent them in monomial form, let

$$M_r := [m_{\nu,\mu}]_{\nu+\mu \le r}, \quad m_{\nu,\mu}(x, y) := x^\nu y^\mu,$$

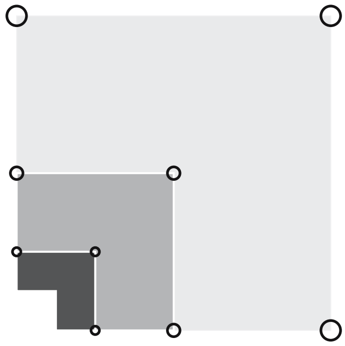

Fig. 7.4 Illustration of (7.29/150): Hermite sampling at the marked points determines the rings.

span the space $\mathbb{P}_r$ of bivariate polynomials of total degree $\le r$. It is convenient to define the algorithm by means of a diagonal matrix J and a corresponding system F of eigenrings. Let $F = [f_{\nu,\mu}]_{\nu+\mu\le r}$ be the set of rings $f_{\nu,\mu} \in C^k(\mathbf{S}_n^0, \mathbb{R}, \tilde{G})$ interpolating the reparametrized monomials $\mathcal{R}_0^{-1}[m_{\nu,\mu}]$ up to order $(3,3)$ at the points $\mathbf{s}_j^i$,

$$\mathcal{H}\big[f_{\nu,\mu} - \mathcal{R}_0^{-1}[m_{\nu,\mu}]\big](\mathbf{s}_j^i) = 0, \quad i = 1,\dots,4,\ j \in \mathbb{Z}_n.$$

According to the labelling of generating rings $f_{\nu,\mu}$, the vector of initial data has the form $\mathbf{P} := [\mathbf{p}_{\nu,\mu}]_{\nu+\mu\le r}$ so that

$$\mathbf{x}^0 = F\mathbf{P} = \sum_{\nu=0}^{r}\sum_{\mu=0}^{r-\nu} f_{\nu,\mu}\mathbf{p}_{\nu,\mu}.$$

Since the values of a monomial $m_{\nu,\mu}$ on $\lambda^m \boldsymbol{\Omega}$ and on $\lambda^{m+1}\boldsymbol{\Omega}$ are related by a scale factor $\lambda^{\nu+\mu}$, and since this monomial corresponds to the rings $f_{\mu,\nu}$, Guided subdivision can be defined by a simple scaling process. We define the diagonal matrix

$$J := \operatorname{diag}\big([\lambda^{\nu+\mu}]_{\nu+\mu\le r}\big)$$

to obtain the recursion

$$\mathbf{x}^m := F\mathbf{P}^m, \quad \mathbf{P}^m := J^m\mathbf{P} = [\lambda^{m(\nu+\mu)}\mathbf{p}_{\nu,\mu}]_{\nu+\mu\le r}.$$

Although this is needed neither for the analysis nor for an implementation, we briefly discuss a possible conversion of the setup into a subdivision algorithm (A, G) in its genuine form. Let $B_r = [b_{\nu,\mu}]_{\nu+\mu\le r}$ denote the vector of bivariate *Bernstein polynomials* of total degree $\le r$ on the unit triangle. Because these Bernstein polynomials are linearly independent, monomials can be represented as linear combinations of them. That is, there exists an invertible matrix V with $M_r = B_r V$ and

$B_r = M_r V^{-1}$. Then we define

$$G := FV^{-1}, \quad \mathbf{Q} := V\mathbf{P}, \quad A := VJV^{-1},$$

to obtain

$$\mathbf{x}^m = FJ^m\mathbf{P} = GA^m\mathbf{Q}.$$

Because the elements $g_{\nu,\mu}$ of the generating system G are Hermite interpolants to the Bernstein polynomials, they form a partition of unity. Further, A represents just de Casteljau's algorithm with scale factor λ,

$$B_r(\lambda\xi)\mathbf{Q} = B_r(\xi)A\mathbf{Q}, \quad \xi = (x, y),$$

showing that the rows of A sum to 1.

Definition 7.25 (Guided $C^{2,7}_{2,r}$-subdivision). For $r \geq 2$, the subdivision algorithm (A, G) with A and G as defined above is called *Guided $C^{2,7}_{2,r}$-subdivision*. The polynomial

$$\mathbf{g} := \bigcup_{m\in\mathbb{N}_0} \lambda^m \boldsymbol{\Omega} \ni \xi \mapsto B_r(\xi)\mathbf{Q} \in \mathbb{R}^d$$

is called the *guide* to the initial data $\mathbf{Q}$.

Although the minimal value $r = 2$ is impeccable from a theoretical point of view, one typically chooses much larger values for r to define a space of rings which covers a sufficiently rich variety of shapes. Let us discuss some implications of the above definition.

First, the subdivision matrix A and the diagonal matrix $J = V^{-1}AV$ are similar so that we can easily read off the common spectrum and see that the structure of the leading eigenvalues is just right.

Second, because J is diagonal, we have

$$\mathbf{x}^m = FJ^m\mathbf{P} = \sum_{\nu=0}^{r}\sum_{\mu=0}^{r-\nu} \lambda^{m(\nu+\mu)} m_{\nu,\mu}\mathbf{p}_{\nu,\mu},$$

showing that $\mathbf{x}^m$ interpolates the reparametrization of $\mathbf{g}_{|\lambda^m\boldsymbol{\Omega}}$,

$$\mathcal{H}\big[\mathbf{x}^m - \mathcal{R}_m^{-1}[\mathbf{g}]\big](\mathbf{s}_j^i) = \sum_{\nu=0}^{r}\sum_{\mu=0}^{r-\nu} \lambda^{m(\nu+\mu)}\mathbf{p}_{\nu,\mu}\mathcal{H}[f_{\nu,\mu} - R_0^{-1}m_{\nu,\mu}](\mathbf{s}_j^i) = 0.$$

Hence, by the chain rule,

$$D_1^\alpha D_2^\beta \mathbf{x}^m(\mathbf{s}_j^1) = 2^{\alpha+\beta} D_1^\alpha D_2^\beta \mathbf{x}^{m+1}(\mathbf{s}_j^2)$$
$$D_1^\alpha D_2^\beta \mathbf{x}^m(\mathbf{s}_j^3) = 2^{\alpha+\beta} D_1^\alpha D_2^\beta \mathbf{x}^{m+1}(\mathbf{s}_j^4)$$

for $(\alpha, \beta) \leq (3, 3)$. Since, for $\ell \leq 2$,

$$D_1^\ell \mathbf{x}^m(1, \cdot, j),\ D_2^\ell \mathbf{x}^m(\cdot, 1, j),\ D_1^\ell \mathbf{x}^{m+1}(2, \cdot, j),\ D_2^\ell \mathbf{x}^{m+1}(\cdot, 2, j)$$

are all polynomials of degree at most 7, we conclude that coincidence of partial derivatives at the points $\mathbf{s}^i_j$ implies

$$D_1^\ell \mathbf{x}^m(1/2,\cdot,j) = 2^\ell D_1^\ell \mathbf{x}^{m+1}(1,\cdot,j)$$
$$D_2^\ell \mathbf{x}^m(\cdot,1/2,j) = 2^\ell D_2^\ell \mathbf{x}^{m+1}(\cdot,1,j).$$

This shows that consecutive rings join C^2 so that Guided subdivision (A,G) is indeed a C^2-algorithm.

Third, the surfaces $\mathbf{x}$ and $\mathbf{g}$ have third-order contact at the points $2^{-m}\mathbf{s}^i_j$. In particular, the points

$$\mathbf{x}(2^{-m}\mathbf{s}^i_j) = \mathbf{g}(\lambda^m \boldsymbol{\xi}^i_j), \quad \boldsymbol{\xi}^i_j := \boldsymbol{\varphi}(\mathbf{s}^i_j)$$

and also the embedded Weingarten maps

$$\mathbf{W}_\mathbf{x}(2^{-m}\mathbf{s}^i_j) = \mathbf{W}_\mathbf{g}(\lambda^m \boldsymbol{\xi}^i_j)$$

coincide. This property accounts for our initial statement, saying that the image of $\mathbf{g}$ yields a good approximation of the image of $\mathbf{x}$. As one approaches the center, the interpolation points become denser and denser so that the shapes are closer and closer.

While the latter observation is relevant for a qualitative assessment of shape, the next theorem verifies analytic smoothness.

Theorem 7.26 (Guided $C^{2,7}_{2,r}$-subdivision works). *For $r \geq 2$, Guided $C^{2,7}_{2,r}$-subdivision (A,G) defines a $C^{2,7}_2$-algorithm.*

Proof. For $\nu + \mu \leq 2$, the ring $\mathcal{R}_0^{-1}[m_{\nu,\mu}]$ lies in $C^2(\mathbf{S}^0_n, \mathbb{R}, G)$, and hence $f_{\nu,\mu} = \mathcal{R}_0^{-1}[m_{\nu,\mu}]$. Since J is a diagonal matrix, we can easily read off the non-zero eigenvalues $\lambda^{\nu+\mu}$, and see that the functions $f_{\nu,\mu}$ are the corresponding eigenrings. The eigenring to the dominant eigenvalue $\lambda_0 = \lambda^0 = 1$ is

$$f_{0,0} = \mathcal{R}_0^{-1}[m_{0,0}] = 1,$$

the eigenrings to the subdominant eigenvalue $\lambda_1 = \lambda_2 = \lambda$ are

$$[f_{1,0}, f_{0,1}] = \mathcal{R}_0^{-1}[m_{1,0}, m_{0,1}] = \boldsymbol{\varphi},$$

and the eigenrings to the subsubdominant eigenvalue $\lambda_3 = \lambda_4 = \lambda_5 = \lambda^2$ are

$$[f_{2,0}, f_{1,1}, f_{0,2}] = \mathcal{R}_0^{-1}[m_{2,0}, m_{1,1}, m_{0,2}] = [f^2_{1,0}, f_{1,0}f_{0,1}, f^2_{0,1}].$$

All other eigenvalues are, by construction, smaller so that the claim follows from Theorem 7.16/143. □

Guided $C^{2,7}_{r,2}$-subdivision fits the pattern of the PTER-framework. The extension process yields the guide $\mathbf{g}$ restricted to the domain $\lambda\boldsymbol{\Omega}$, while the projecting step into the appropriate space is defined via Hermite sampling at the points $\boldsymbol{\xi}^i_j$.

Bibliographical Notes

1. The importance of the ratio $\varrho := \frac{\mu}{\lambda^2}$, as defined in (7.14/130), was already observed in the early days of subdivision, and the search for good algorithms was sometimes guided by aiming at the optimal value $\varrho = 1$ [DS78, Loo87]. It was even conjectured (but of course soon disproven) that $\varrho = 1$ was *sufficient* for curvature continuity [BS90, Sto85]. Necessary conditions for boundedness of curvatures were discussed by Holt in [Hol96]. However, a rigorous proof must exclude degeneracy for generic initial data in the sense of Lemma 7.5/132. This proof appears first in [Rei07].

2. Algorithms generating surfaces with bounded curvature include those of Sabin [Sab91a], Holt [Hol96] and Loop [Loo02a], as well as the C^2-subdivision surfaces with enforced flat spots introduced by Prautzsch and Umlauf [PU98a, PU98b, PU00b], see remark after Theorem 7.15/141. Bounds on the curvature for such algorithms are derived by Peters and Umlauf in [PU01] based on tools for the analysis of the Gauss and mean curvature of subdivision surfaces in [PU00a].

3. The asymptotic expansions in Sect. 7.1/126 and most of the material in Sect. 7.2/134 follow ideas developed in [PR04]. In particular, the concept of the central ring, see Definition 7.2/128, is introduced there.

4. An alternative measure for assessing the variety of shapes that can be generated by a subdivision algorithm is 'r-flexibility', as introduced in [PR99].

5. Amazingly, the inability of the standard Catmull–Clark algorithm to generate convex shape for $n \geq 5$, as explained by Theorem 7.10/136, was not discovered before [PR04]. A detailed study of shape properties and suggestions for tuning Catmull–Clark subdivision can be found in [KPR04].

6. Theorem 7.6/132 is due to Reif and Schröder [RS01]. It is essential for using subdivision surfaces for Finite element simulation of thin shells and plates [CSA$^+$02, COS00].

7. While the original paper by Karčiauskas, Peters and Reif [KPR04] used n-sided *shape charts*, Augsdörfer, Dodgson and Sabin [ADS06] switched to equivalent circular charts. Hartmann [Har05] as well as Ginkel and Umlauf [GU08] took advantage of symmetries to reduce the chart to one sector for even valences and a half-sector for odd valences. Shape charts have been used to improve the curvature behavior at the central point [ADS06, GU06a, GU06b, GU07b]. Ginkel's thesis points out the remarkable fact that a large class of algorithms cannot handle high-valence satisfactorily: no matter how the input data are adjusted, there is no purely convex or a purely hyperbolic neighborhood of the singularity.

8. The C_2^k-criterion of Theorem 7.16/143 appears in similar form in [Pra98]. In [BK04], Barthe and Kobbelt propose tuning subdivision to approximate the conditions of the theorem.

9. Sabin [Sab91a] is the first to argue that Catmull–Clark and other piecewise bicubic algorithms that generate C^2-rings cannot be C^2 at the central point. The precise degree estimate Theorem 7.19/144 is due to Reif [Rei96a]. It is valid not only

for stationary algorithms, but for any scheme generating piecewise polynomial surfaces with the given structure of rings. Generalized degree estimates can be found in [PR99]. A stunning circumvention of the seemingly solid degree barrier has recently been discovered by Karčiauskas and Peters [KP05]. The idea is to increase the number of segments when approaching the singularity.

10. The first C_2^k-subdivision algorithms where constructed by Reif [Rei96b, Rei98] for TURBS, and by Prautzsch [Pra97] for Freeform splines. Although being impeccable from a theoretical point of view, both algorithms failed to gain much popularity. While, for TURBS, this is easily explained by a substantial lack of visual fairness, Freeform splines should have deserved better.

11. The Guided subdivision of Karčiauskas and Peters [KP05, KP07b, KMP06] is based on a fundamental revision and generalization of the ideas behind TURBS and Freeform splines. It combines analytical smoothness with high visual fairness, and should be considered a prototype for a new generation of premium algorithms. The development of the general PTER-framework, at present unpublished, was inspired by the concept of Guided subdivision. In particular, the proof of Lemma 7.22/146 uses ideas appearing already in [KMP06].